51 copies

NATIONAL AERONAUTICS AND SPACE ADMINISTRATION

Technical Report 32-1066

Precision Power Measurements of Spacecraft CW Signal With Microwave Noise Standards

C. T. Stelzried
M. S. Reid
D. Nixon

JET PROPULSION LABORATORY
CALIFORNIA INSTITUTE OF TECHNOLOGY
PASADENA, CALIFORNIA

February 15, 1968

NATIONAL AERONAUTICS AND SPACE ADMINISTRATION

Technical Report 32-1066

Precision Power Measurements of Spacecraft CW Signal With Microwave Noise Standards

C. T. Stelzried
M. S. Reid
D. Nixon

Approved by:

G. S. Levy, *Manager*
Communications Elements Research Section

JET PROPULSION LABORATORY
CALIFORNIA INSTITUTE OF TECHNOLOGY
PASADENA, CALIFORNIA

February 15, 1968

TECHNICAL REPORT 32-1066

Prepared Under Contract No. NAS 7-100
National Aeronautics & Space Administration

PRECEDING PAGE BLANK NOT FILMED.

Acknowledgment

The *Mariner IV* power calibration project was suggested by W. K. Victor, and encouraged by P. Potter and W. Higa. Most of the measurements were performed by Goldstone station personnel and the authors wish to express their appreciation especially to N. Proebstel, at the Pioneer station, and A. Hull and T. Miller, at the Echo station. R. A. Gardner and K. B. Wallace constructed the special narrow-band filters.

Contents

Contents (contd)

Tables

Figures

Contents (contd)

Figures (contd)

Abstract

Determination of the absolute level of the received CW power is one of the important measurements required in the evaluation of a spacecraft communications system. A new, precise measurement method that compares CW signal power with microwave noise power is described. This technique, together with statistical methods of data reduction, results in significantly increased accuracy. The overall probable error of the measurement was reduced from 0.8 to 0.3 dB defined at the receiver input for an antenna receiving system at the JPL Goldstone Deep Space Communications Complex. Application of these techniques to *Mariner IV* began on June 29, 1965, and was continued after Mars encounter. The theory, equipment, and method of data acquisition and reduction are described, and results and accuracies are discussed. The *Mariner IV* received power at Mars encounter normalized for 100% antenna efficiency was −154.2 dBmW, as compared to a theoretically predicted level of −153.1 dBmW.

Precision Power Measurements of Spacecraft CW Signal With Microwave Noise Standards

I. Introduction

The determination of the CW power level received from spacecraft is required in the experimental evaluation of the communications system of a deep space mission. This measurement is important for the design of future spacecraft as well as for the evaluation of earth-bound receiving stations. A new and improved technique of measuring spacecraft power levels that results in significantly reduced errors is described in this report.

Mariner IV was launched from Cape Kennedy on November 28, 1964, on a 228-day mission to Mars. It achieved its closest approach to Mars, approximately 6000 mi, on July 14, 1965, and continues to orbit the sun once every 570 days. Calibrations of the *Mariner IV* received power by this new method were initiated on June 29, 1965, and continued after Mars encounter. The theory, equipment, calibrations, data measurement, and analysis are described herein.

The experiment was performed at two independent stations at the Goldstone Deep Space Communications Complex (GDSCC), requiring a basis for comparison of the results by a normalization process. This report establishes a basis for comparison and discusses the required antenna gain measurements. The measurements from the Goldstone Pioneer and Echo stations (85-ft antennas) of *Mariner IV* power, at Mars encounter, are averaged and compared with the predicted value.

The computer program is included in Appendix A of this report and discussed in Appendix B. The diode correction factor is treated in Appendix C. Appendix D is a flow chart of the computer program.

II. Ground Receiving System and DSIF Standard or Nominal Method of CW Power Calibrations

A simplified block diagram of a standard Deep Space Network (DSN) receiving system is shown in Fig. 1. A convenient measure of the received spacecraft power in a ground-tracking station is the receiver AGC voltage, which is calibrated for absolute received power, defined at the receiver input, with a calibrated test transmitter.

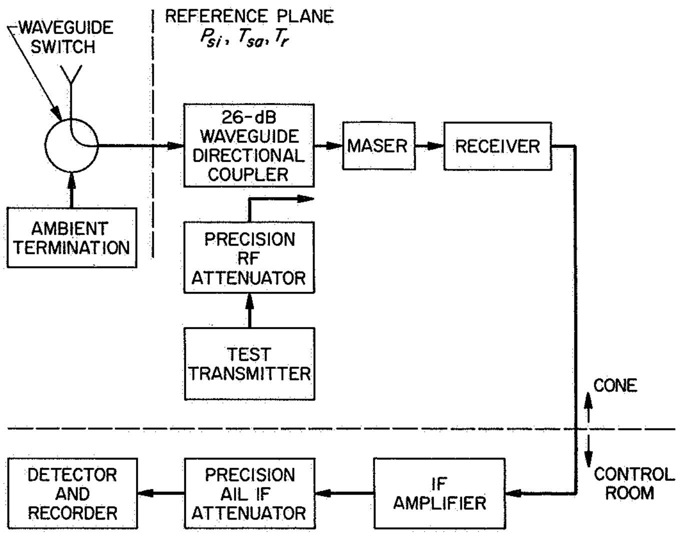

Fig. 1. Simplified block diagram of a standard ground station receiving system

The power output of the test transmitter is adjusted with a precision RF attenuator. The relative accuracy of this adjustment primarily depends on the RF attenuator. The absolute calibration accuracy, however, depends not only on the precision RF attenuator, but also on the calibration of the insertion loss between the RF attenuator and the receiver input reference plane. This insertion loss measurement is extremely difficult to perform. The transmission line path includes coaxial switches, coaxial-to-waveguide transitions, and a 26-dB waveguide directional coupler. The transmission line loss between test transmitter and receiver input can be calibrated only when sufficient station shut-down time is available.

The daily pretracking calibration of a nominal AGC curve relates receiver AGC voltage to a nominal signal input power defined at the receiver input reference plane. Later, typically 1 or 2 h after the determination of this AGC curve, the spacecraft signal is acquired by the station and the receiver AGC voltage is noted. The AGC curve then yields a nominal value for the spacecraft CW power. The AGC curve is also re-evaluated during the post-tracking calibrations.

The results of a detailed error analysis (see Subsection IV-B-9) predicted that, with this nominal technique, spacecraft power, defined at the receiver reference plane, can be measured with an overall probable error of approximately 0.8 dB for a single measurement (Ref. 1). This error of 0.8 dB is the theoretical lower limit of probable error for the nominal measurement method. In practice, the nominal probable error may be in excess of this figure.

III. The Noise Power Comparison Method of CW Power Measurements

A. Theory

The test transmitter signal power can be calibrated directly at the receiver input reference plane without insertion loss measurement by the Y-factor technique of power ratio measurements used in noise temperature calibrations. The method compares the test transmitter CW power with the receiving system noise power, which can be determined accurately with calibrated microwave thermal terminations. The total power, contained in the system noise P_n, plus the CW power P_s, is compared at the output of the receiving system with the system noise power alone. The precision IF attenuator is adjusted for equal power levels with the CW power on and off. This Y-factor power ratio is given by

$$Y = \frac{P_n + P_s}{P_n} \tag{1}$$

The noise power, P_n, observed at the detector input, is a function of the overall system gain $G(f)$ (Ref. 2), as follows:

$$P_n = kT_s \int_0^\infty G(f)\, df \tag{2}$$

where

T_s = system's temperature, defined at the receiver input reference plane, °K

k = Boltzmann's constant, J/°K

The signal power, P_s, observed at the detector input, is a function of the input signal power, P^*_{si}, defined at the receiver input reference plane, and the overall gain $G(f_s)$ at the signal frequency, f_s,

$$P_s = P^*_{si} \cdot G(f_s) \tag{3}$$

Substituting Eqs. (2) and (3) into Eq. (1), normalizing with

$$g(f_s) = \frac{G(f_s)}{G(f_0)} \tag{4}$$

where $G(f_0)$ is defined as the maximum gain, and defining noise bandwidth (Ref. 3) as

$$B = \frac{1}{G(f_0)} \int_0^\infty G(f)\, df \tag{5}$$

This results in

$$p^*_{si} = \frac{(Y-1)\,kT_s B}{g(f_s)} \tag{6}$$

Because the detector in the receiving system uses a semiconductor diode whose output is a function of input signal form factor, a correction term is required in Eq. (6) to account for the diode's noise vs CW power sensitivity. Therefore, Eq. (6) is rewritten as

$$P^*_{si} = \frac{\alpha (Y-1)\,kT_s B}{g(f_s)} \tag{7}$$

where

α = the diode correction factor

With measurements of Y, B, T_s, α, and $g(f_s)$, the input CW power from the test transmitter is calculated from Eq. (7). This is used to provide a correction to the nominal AGC curve. The calibrated spacecraft power, P_{si}, is obtained by applying this correction to the measured nominal spacecraft power.

With an antenna efficiency η, defined at the receiver input, the power incident on the antenna is

$$P'_{si} = \frac{P_{si}}{\eta} \tag{8}$$

and, with an atmospheric loss L, the incident power outside the earth's atmosphere is

$$P''_{si} = (P'_{si})\,(L_0)^{\sec z} \tag{9}$$

where

z = zenith angle in degrees

Equation (9) is especially useful for power measurement comparison between stations.

B. Error Analysis and Limitations

The error in the test transmitter input signal power calibration can be determined from an error analysis of Eq. (7). The probable error $PE_{P_{si}}$ is

$$\begin{aligned}(PE_{P^*_{si}})^2 = {} & \left(\frac{\partial P^*_{si}}{\partial Y}\right)^2 (PE_Y)^2 + \left(\frac{\partial P^*_{si}}{\partial T_s}\right)^2 (PE_{T_s})^2 \\ & + \left(\frac{\partial P^*_{si}}{\partial B}\right)^2 (PE_B)^2 + \left(\frac{\partial P^*_{si}}{\partial g(f_s)}\right)^2 (PE_{g(f_s)})^2 \\ & + \left(\frac{\partial P^*_{si}}{\partial \alpha}\right)^2 (PE_\alpha)^2 \end{aligned} \tag{10}$$

which may be written (Ref. 4)

$$\begin{aligned}\left(\frac{PE_{P^*_{si}}}{P^*_{si}}\right)^2 = {} & \left(\frac{PE_Y}{Y}\right)^2 \left(1 + \frac{\alpha k T_s B}{P^*_{si}\, g(f_s)}\right)^2 + \left(\frac{PE_{T_s}}{T_s}\right)^2 \\ & + \left(\frac{PE_B}{B}\right)^2 + \left(\frac{PE_{g(f_s)}}{g(f_s)}\right)^2 + \left(\frac{PE_\alpha}{\alpha}\right)^2 \end{aligned} \tag{11}$$

The probable error ratio, PE_Y/Y, in the Y-factor measurements, is primarily a function of:

(1) The resetability and nonlinearity of the IF attenuator and null indicator. These error contributions may be written as a_1^2 and $(a_2 Y_{dB})^2$, where a_1 and a_2 are the resetability and linearity constants obtained from the manufacturer's specification.

(2) Receiver gain instability. This error contribution is (Ref. 5)

$$\left[\frac{1}{\tau B} + \left(\frac{\Delta G}{G_0}\right)^2\right]^{1/2}$$

where

τ = post-detector time constant

$\frac{\Delta G}{G_0}$ = statistical overall receiver gain ratio fluctuations

(3) The test transmitter input CW power ratio instability $\Delta P^*_{si}/P^*_{si}$ during the time of the Y-factor measurement (Eq. 1).

Thus,

$$\left(\frac{PE_Y}{Y}\right)^2 = a_1^2 + (a_2 Y_{dB})^2 + \frac{1}{\tau B} + \left(\frac{\Delta G}{G_0}\right)^2 + \left(\frac{\Delta P^*_{si}}{P^*_{si}}\right)^2 \tag{12}$$

Figure 2 illustrates the normalized probable error ratio $PE_{P^*_{si}}/P^*_{si}$ versus P^*_{si} in dBmW for two values of bandwidth and time constant:

$$B_1 = 10.0\,\text{kHz} \qquad \tau_1 = 0.1\,\text{s}$$

$$B_2 = 1.0\,\text{kHz} \qquad \tau_2 = 1.0\,\text{s}$$

and for the following parameters:

$$PE_B/B = 0.0026\,\text{dB}$$

$$PE_{g(f_s)}/g(f_s) = 0.003\,\text{dB}$$

$$T_s = 45°\text{K}$$

$$k = 1.38054 \times 10^{-23}\,J/°\text{K}$$

$$\frac{\Delta P^*_{si}}{P^*_{si}} = 0.005\,\text{dB}$$

$$\frac{\Delta G}{G_0} = 0.005\,\text{dB}$$

$$PE_{T_s}/T_s = 0.008\,\text{dB}$$

$$PE_\alpha = 0.1\,\text{dB}$$

$$g(f_s) = 1.0\,\text{dB}$$

$$a_1 = 0.003\,\text{dB}$$

$$a_2 = 0.004\,\text{dB}$$

Figure 2 shows that maximum resolution at low power levels is obtained by narrowing the bandwidth and increasing the post-detector time constant. Sufficient resolution cannot be obtained at low input power levels with the standard DSN station bandwidth of approximately 1 MHz. Therefore, the addition of a narrow-band filter was required for the test-transmitter calibrations. The post-detector time constant must be short enough to render the effect of system drifts and gain changes, which are proportional to elapsed time, negligible during the Y-factor measurement. The optimum bandwidth, consistent with a suitable time constant, the power levels measured, and manufacturer's capability, was approximately 10 kHz for JPL requirements.

The error terms in Eq. (11) were analyzed in detail for each station's instrumentation. Calibration errors of the test transmitter are approximately 0.13 dB. Further instrumentation errors, common to the DSIF nominal and

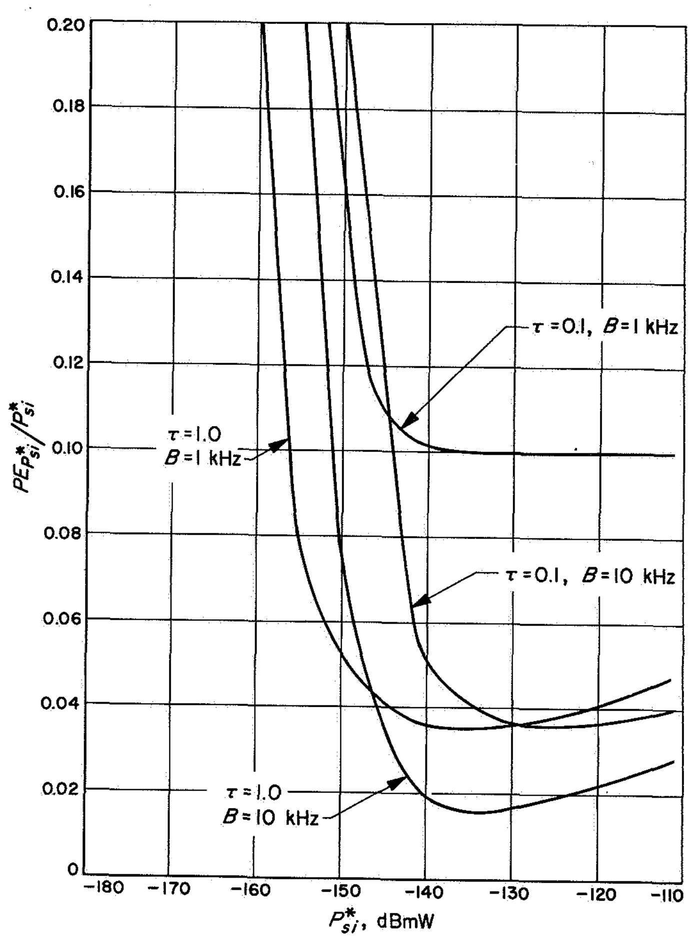

Fig. 2. CW signal power measurement resolution vs signal level

the new noise-calibration methods, resulted in a theoretically predicted overall spacecraft power measurement probable error of approximately 0.3 dB for a single measurement, defined at the receiver input, for a station. These common sources of error are AGC curve inaccuracies (measurement scatter), test transmitter attenuation nonlinearities, antenna misalignment, and spacecraft AGC voltage uncertainties.

C. Equipment

The narrow-band filter consists of a temperature-regulated crystal filter, an IF amplifier, and a 1-MHz bandwidth bandpass filter. This equipment is mounted on a standard 19-in. × 4.5-in. panel (Fig. 3). A circuit diagram of the panel is presented in Fig. 4. The 1-MHz bandpass filter eliminates spurious frequency responses outside the normal bandwidth of the crystal filter. The narrow-band filter essentially determines the operating noise bandwidth of the system. The panel is inserted into the standard DSN system, as required, with coaxial cables.

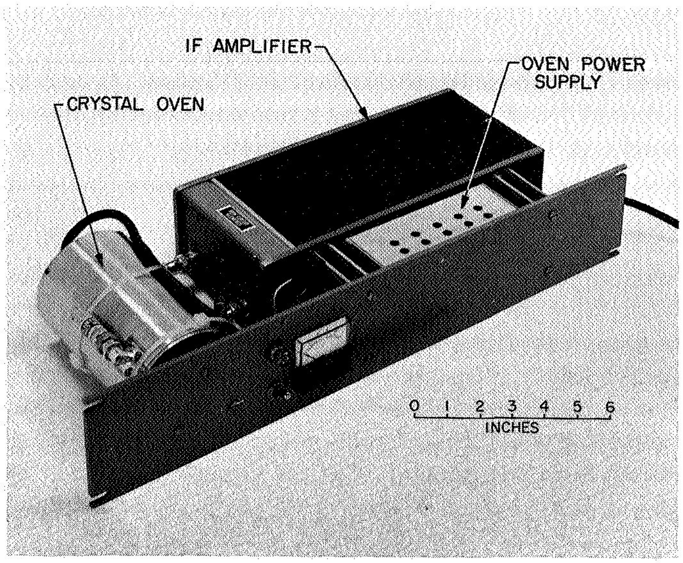

Fig. 3. Filter and amplifier unit

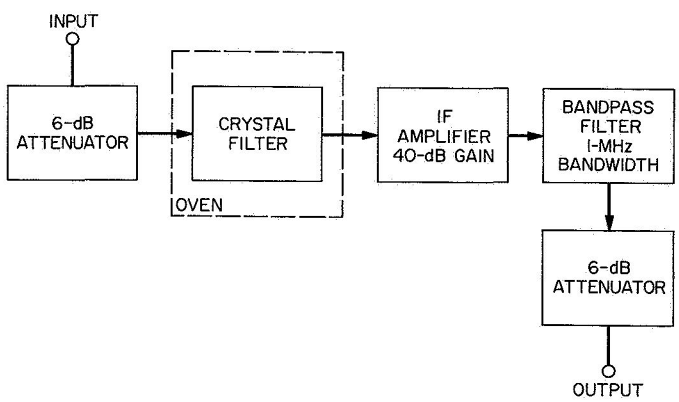

Fig. 4. Block diagram of filter and amplifier unit

This panel is the only equipment required in addition to the standard DSN ground station. Typical narrow-band filter specifications are:

Parameter	Specification
Oven temperature	50°C
Center frequency	50 MHz
3-dB bandwidth	5 kHz
50-dB bandwidth	25 kHz
All responses outside ±25 kHz	50 dB down
Overall dimensions	1.5-in. diam × 2.5-in. height

D. Calibration

1. Bandwidth. Filter bandwidth, as defined by Eq. (5), was evaluated by measuring gain as a function of frequency over a sufficient number of data points (Fig. 5). The data were integrated numerically on a computer to yield total bandwidth. Total filter bandwidth is given by (Ref. 4):

$$B = \int_0^\infty y_i \, df$$

$$\approx \frac{1}{2} y_1 (f_2 - f_1) + \left[\frac{1}{2} \sum_{i=2}^{n-1} y_i (f_{i+1} - f_{i-1}) \right] + \frac{1}{2} y_n (f_n - f_{n-1}) \qquad (13)$$

where

B = bandwidth, Hz

f_i = frequency of i^{th} data point, Hz

y_i = relative gain corresponding to frequency f_i, ratio

n = number of data points

Several sets of data were taken and an average found for each filter. The bandwidth of each station's filter was evaluated periodically in this manner over the period during which the spacecraft CW power was calibrated. Filter bandwidth was not constant with time, but changed slowly, probably because of crystal aging. The filter

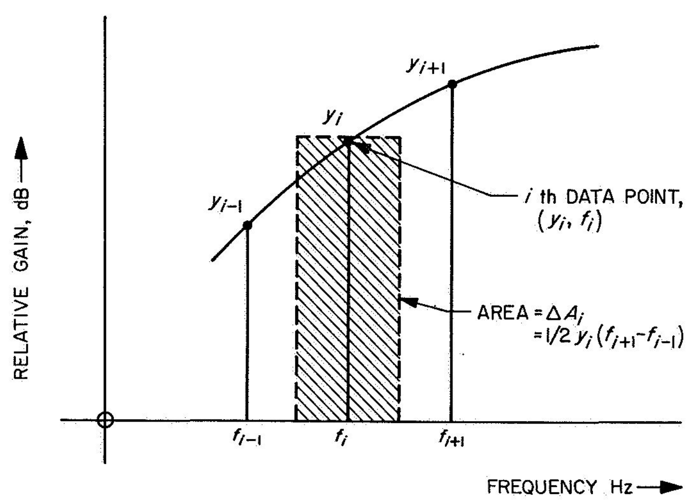

Fig. 5. The measurement of bandwidth by trapezoidal integration

bandwidths for the period of interest were: (1) Pioneer (DSS 11): 11.455 kHz; and (2) Echo (DSS 12): 9.721 kHz.

An error analysis of Eq. (13) was performed (Ref. 4). If PE_B is the probable error in total integrated bandwidth in hertz, then

$$(PE_B)^2 = \sum_{i=1}^{n} (PE_{y_i})^2 \left(\frac{\partial B}{\partial y_i}\right)^2 + \sum_{i=1}^{n} (PE_{f_i})^2 \left(\frac{\partial B}{\partial f_i}\right)^2 \tag{14}$$

where

PE_{y_i} = probable error of the i^{th} attenuation reading, ratio

PE_{f_i} = probable error of the i^{th} frequency reading, Hz

If PE_{f_i} is considered constant for all data points, then Eq. (14) can be expanded as

$$\left(\frac{PE_B}{B}\right)^2 = \frac{1}{4B}\Bigg\{[a_1^2 + (a_2 Y_1)^2]\left(\frac{\ln 10}{10}\right)^2 (f_2 - f_1)^2 y_1^2 + \sum_{i=2}^{n-1} [a_1^2 + (a_2 Y_i)^2]\left(\frac{\ln 10}{10}\right)^2 (f_{i+1} - f_{i-1})^2 y_i^2 + [a_1^2 + (a_2 Y_n)^2]\left(\frac{\ln 10}{10}\right)^2 (f_n - f_{n-1})^2 y_n^2 + (PE_f)^2 (y_1^2 + y_n^2) + (PE_f)^2 \sum_{i=2}^{n-1} (y_{i-1} - y_{i+1})^2\Bigg\} \tag{15}$$

where

a_1 and a_2 = the attenuator constants referred to above

$Y_i = y_i$ in decibel

PE_B/B = the normalized bandwidth probable error

Equations (13) and (15) were programmed in Fortran and the bandwidth data reduced by computer. The average probable error in B for the sources of error investigated was 25 Hz, which contributes approximately 0.01 dB to the test transmitter calibration error.

2. *Diode detector correction factor.*

a. Method and equipment. Since the output of the detector shown in Fig. 1 (a solid-state germanium diode 1N198) is affected by the signal form factor, an evaluation of the diode noise versus CW power sensitivity was required (Ref. 6). The correction factor α (see Eq. 7) was determined by comparison of Y-factors, Y_d and Y_p, measured with the diode and a true rms detector, respectively, at the same signal-to-noise ratio.

The overall equivalent noise bandwidths with the rms detector and the diode had to be equalized to obtain meaningful results. The rms detector was a standard thermistor power meter which, compared with the diode, required a relatively high-input power level for an accurate readout. This high-noise power requirement called for an equalization of diode and power meter bandwidths, as well as equal shape factors, over a large dynamic range. Because, in practice, this is extremely difficult to achieve, the method adopted was to approximate equal bandwidths, accurately evaluate them over a sufficiently wide range of frequencies and attenuations, and apply a correction factor.

A block diagram of the Y-factor comparison test system is presented in Fig. 6. A low-pass filter was required in the power meter circuit to limit the bandwidth. The input could be switched between a signal generator at the RF frequency, 2295 MHz, and a matched termination. The term G_1 is the gain provided by a chain of wide-band transistor amplifiers centered at the IF frequency, A is the attenuation provided by a precision IF attenuator, and the narrow-band filter is that mentioned in the introduction to Subsection III-C. The amplifier chain G_1, resistively terminated on the input, provided the noise power. First, a Y-factor was measured with the diode as the detector; the same Y-factor was then measured with the power meter as the detector. A large number of Y-factors were measured with signal-to-noise ratios in the range

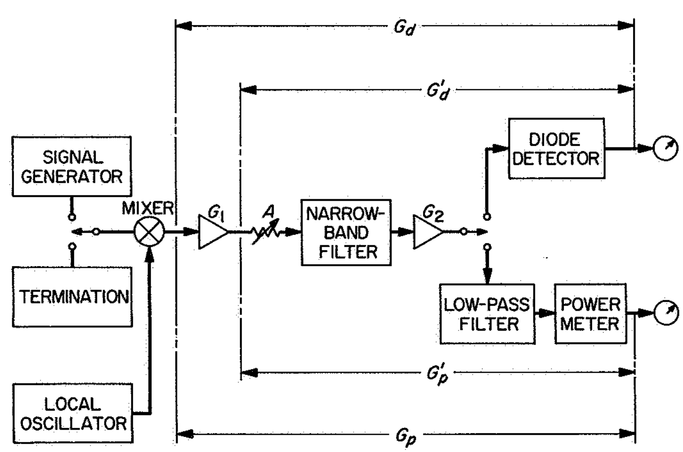

Fig. 6. Block diagram for diode sensitivity evaluation

1 to 30 dB. The measurements were repeated for different diode bias levels.

b. Theory. With the gain notation shown in Fig. 6, the diode and rms detector Y-factors can be defined as (Ref. 6):

$$Y_d = 1 + \frac{P^*_{si} G_d(f_s)}{\alpha k T_s \int_0^\infty G_d(f)\,df} \tag{16}$$

$$Y_p = 1 + \frac{P^*_{si} G_p(f_s)}{k T_s \int_0^\infty G_p(f)\,df} \tag{17}$$

where

α = diode correction factor, ratio

P^*_{si} = input power, W

f_s = signal frequency, Hz

T_s = system temperature, °K

Solving Eqs. (16) and (17) for α gives:

$$\alpha = \frac{Y_p - 1}{Y_d - 1}\,\frac{G_d(f_s)}{G_p(f_s)}\,\frac{\int_0^\infty G_p(f)\,df}{\int_0^\infty G_d(f)\,df} \tag{18}$$

Equation (18) may be normalized with the following two sets of equations:

$$\left.\begin{aligned} \frac{G_d(f_s)}{G_{d0}} &= g_d(f_s) \\ \frac{G_p(f_s)}{G_{p0}} &= g_p(f_s) \end{aligned}\right\} \tag{19}$$

and

$$\left.\begin{aligned} \frac{G_d(f)}{G_{d0}} &= g_d(f) \\ \frac{G_p(f)}{G_{p0}} &= g_p(f) \end{aligned}\right\} \tag{20}$$

where the subscript 0 refers to the point of maximum gain. After normalization with Eqs. (19) and (20), Eq. (18) yields

$$\alpha = \frac{Y_p - 1}{Y_d - 1}\,\frac{g_d(f_s)}{g_p(f_s)}\,\frac{\int_0^\infty g_p(f)\,df}{\int_0^\infty g_d(f)\,df} \tag{21}$$

However, since

$$\int_0^\infty g_d(f)\,df = \text{overall equivalent noise bandwidth with diode}$$

and

$$\int_0^\infty g_p(f)\,df = \text{overall equivalent noise bandwidth with power meter}$$

$$\alpha = \frac{Y_p - 1}{Y_d - 1}\,\frac{g_d(f_s)}{g_p(f_s)}\,\frac{B_p}{B_d} \tag{22}$$

The ratios $b = B_p/B_d$ and $g = g_d(f_s)/g_p(f_s)$ were evaluated by measuring B_p and B_d over a sufficiently wide range of frequencies and attenuations. Equation (22) was then written as

$$\alpha\,(\text{dB}) = 10\log_{10}\left(\frac{Y_p - 1}{Y_d - 1}\,g \cdot b\right) \tag{23}$$

c. Error analysis. An error analysis of Eq. (23) was performed (Ref. 6)

$$[PE_{\alpha(\text{dB})}]^2 = (10\log_{10} e)^2\left[\left(\frac{PE_{Y_p}}{Y_p - 1}\right)^2 + \left(\frac{PE_{Y_d}}{Y_d - 1}\right)^2 + \left(\frac{PE_g}{g}\right)^2 + \left(\frac{PE_b}{b}\right)^2\right] \tag{24}$$

However, since

$$Y_p(\text{dB}) = 10\log_{10} Y_p$$

and

$$PE_{Y_p} = \left[\frac{\partial Y_p}{\partial Y_p(\text{dB})}\right] PE_{Y_p}(\text{dB})$$

Equation (24) may be written as

$$[PE_{\alpha(\text{dB})}]^2 = \left(\frac{Y_p}{Y_p - 1}\right)^2 (PE_{Y_{p(\text{dB})}})^2 + \left(\frac{Y_d}{Y_d - 1}\right)^2 \times (PE_{Y_{d(\text{dB})}})^2 + (10\log_{10} e)^2\left[\left(\frac{PE_g}{g}\right)^2 + \left(\frac{PE_b}{b}\right)^2\right] \tag{25}$$

Equations (23) and (25) were programmed in Fortran and the data reduced by computer. The diode correction factor, α, was evaluated for each station with various signal-to-noise ratios and was essentially constant for the signal-to-noise ratios of interest (greater than 10 dB).

A theoretical analysis that verified these results is discussed in Appendix C. The correction factor was different for each diode and was sensitive to ambient temperature and signal level. The corrections for the Pioneer and Echo stations were 0.41 and 0.44 dB, respectively. The error analysis indicated that α was determined with an accuracy that contributed an error of less than 0.1 dB to the test transmitter calibration error.

3. Antenna efficiency.

a. Theory and method. To compare the CW-received signal level at different stations, antenna efficiency must be taken into account. Antenna gain was measured at each station using radio star tracks over an extended period of time, typically 3 or 4 weeks. A Y-factor method of evaluating radio source temperature was chosen because a simple, quick test was required, which would not interrupt normal station operation to any great extent.

Antenna efficiency is given by (Ref. 4):

$$\eta = \frac{\text{Measured source temperature}}{\text{Assumed source temperature}}$$

$$= \left(\frac{T_0 + T_r}{T}\right) \cdot \left(\frac{1}{Y_1} - \frac{1}{Y_2}\right) \qquad (26)$$

where

η = relative antenna efficiency defined at the receiver input reference plane, ratio

T_0 = temperature of ambient load, °K

T_r = receiver effective noise temperature defined at the receiver input reference plane, °K

T = assumed source temperature, °K

Y_1 = Y-factor, switching receiver input between ambient load and antenna on the radio source, ratio

Y_2 = Y-factor, switching receiver input between ambient load and antenna off the radio source, ratio

Two radio sources, Omega and Taurus A (assumed temperatures of 99 and 132°K, respectively) were chosen, and each station tracked these sources almost nightly for several weeks. To refer antenna efficiency to the antenna input, it would be necessary to measure and account for the transmission line losses between the antenna and the maser input. However, for purposes of this report, where spacecraft power is also measured and defined at the maser input, Eq. (26) results in the proper antenna efficiency for transforming the spacecraft power measurements to the antenna input. Figure 7 shows the format used to record the information at each station. Data taken by the Echo station on August 13, 1965, on Omega, are presented.

Equation (26) yields antenna efficiency, assuming no atmospheric loss. The measured radio source temperature T', assuming a flat earth, is related to the assumed source temperature, T, by

$$T' = T\,(L_0)^{\sec z} \qquad (27)$$

where

L_0 = atmospheric loss at zenith, ratio.

The zenith angle is given by

$$\cos z = \sin\phi \sin\delta + \cos\phi \cos\delta \cos h \qquad (28)$$

where

ϕ = latitude of antenna

δ = radio source declination

h = radio source hour angle

Equations (26) through (28) were programmed in Fortran and the data reduced by computer. Table 1 shows the computer output format for a typical station on Omega. Because measurements taken on any one night were insufficient to evaluate atmospheric loss correctly, an average estimated value was chosen and the data were reduced using this value. Three columns of data are shown in Table 1 for each of the three assumed values of L_0. The best value is probably L_0 = 0.05 dB; the other two values were considered limiting cases. For each assumed value of L_0 and for each set of measurement data, an atmospheric loss in decibels corresponding to the associated zenith angle has been calculated and is shown under the heading L, dB. The other two columns, T and Nu, list the measured source temperature (°K) and antenna efficiency (%) for each corresponding zenith angle. The average efficiency, and standard deviation, for each assumed value of L_0 were calculated and are shown at the bottom of Table 1.

Table 2 presents a summary of all the data. The average antenna efficiency and standard deviation are shown for each station on each source. The best estimate for antenna efficiency is the average of the measurements from Omega and Taurus A for an assumed atmospheric loss at zenith of 0.05 dB. The results are: Pioneer station, 50.0%; and Echo station, 56.2%.

STATION: 12 DATE: 13 AUGUST 1965

1. Track source: OMEGA

2. Boresight

3. While tracking source switch between ambient load and antenna:
   Y_1 (on source): 1. 4.65 db 2. 4.64 db 3. 4.65 db 4. 4.64 db 5. 4.64 db

4. Antenna off source about 3 deg. Switch between ambient load and antenna:
   Y_2 (off source): 6. 7.86 db 7. 7.86 db 8. 7.87 db 9. 7.86 db 10. 7.85 db

5. Temperature on ambient load = 27.8°C

ON SOURCE				OFF SOURCE			
Data point	Time, GMT	Hour angle	Declination	Data point	Time, GMT	Hour angle	Declination
1	074308	045.744	343.848	6	074629	043.574	343.848
2	074340	045.878	343.848	7	074702	043.708	343.848
3	074407	045.990	343.848	8	074729	043.820	343.848
4	074431	046.094	343.848	9	074753	043.918	343.848
5	074500	046.214	343.848	10	074829	044.068	343.848

Y_1 average = 4.644 db = 2.9134 ratio

Y_2 average = 7.860 db = 6.1094 ratio

$$\eta = \frac{273.18 + 27.8 + 11}{99}\left\{\frac{1}{2.9134} - \frac{1}{6.1094}\right\} = 56.59\%$$

Fig. 7. Radio source measurements

Table 1. Antenna system efficiency measurements[a] at station 11 source Omega

Date	Hour angle, deg	Zenith angle, deg	$L_0 = 0$ dB			$L_0 = 0.05$ dB			$L_0 = 0.1$ dB		
			L, dB	T, °K	N_a, %	L_1, dB	T_1, °K	N_{a1}, %	L_2, dB	T_2, °K	N_{a2}, %
7–5–65	12.8	52.895	0.0	47.983	48.46	0.08	48.907	49.40	0.16	49.850	50.35
7–10–65	32.9	60.205	0.0	46.532	47.00	0.10	47.623	48.10	0.20	48.739	49.23
7–20–65	53.2	72.068	0.0	46.282	46.75	0.16	48.046	48.53	0.32	49.876	50.38
7–21–65	26.3	57.230	0.0	52.613	53.14	0.09	53.745	54.28	0.18	54.900	55.45
7–21–65	33.2	60.334	0.0	51.666	52.18	0.10	52.881	53.41	0.20	54.126	54.67
8–3–65	28.9	58.312	0.0	48.428	48.91	0.09	49.501	50.00	0.19	50.598	51.10
8–5–65	30.9	59.215	0.0	47.343	47.82	0.09	48.420	48.90	0.19	49.521	50.02
8–6–65	13.0	52.918	0.0	48.860	49.35	0.08	49.802	50.30	0.16	50.762	51.27
8–6–65	13.6	53.073	0.0	48.925	49.41	0.08	49.872	50.37	0.16	50.837	51.35
8–6–65	43.8	66.112	0.0	48.206	48.69	0.12	49.597	50.09	0.24	51.027	51.54
8–6–65	4.0	51.608	0.0	49.132	49.62	0.08	50.051	50.55	0.16	50.988	51.50
8–6–65	35.9	61.742	0.0	47.311	47.78	0.10	48.475	48.96	0.21	49.669	50.17
8–6–65	27.4	57.675	0.0	48.792	49.28	0.09	49.854	50.35	0.18	50.939	51.45
8–7–65	32.3	59.884	0.0	47.589	48.07	0.09	48.694	49.18	0.19	49.824	50.32
8–8–65	24.2	56.363	0.0	48.011	48.49	0.09	49.019	49.51	0.18	50.049	50.55
8–9–65	47.7	68.526	0.0	47.410	47.88	0.13	48.925	49.41	0.27	50.488	50.99
Efficiency averages, %					48.932			50.089			51.275
Standard deviations, %					1.633			1.585			1.567

[a]Station latitude: 35.281533 deg
Theoretical source temperature = 99°K

b. Error analysis. If PE_η is the probable error of the antenna efficiency, then, from Eq. (26),

$$\left(\frac{PE_\eta}{\eta}\right)^2 = \left(\frac{PE_{T_0}}{T_0}\right)^2\left(\frac{T_0}{T_0+T_r}\right)^2 + \left(\frac{PE_{T_r}}{T_r}\right)^2\left(\frac{T_r}{T_0+T_r}\right)^2 + \left(\frac{PE_{Y_1}}{Y_1}\right)^2\left(\frac{Y_2}{Y_2-Y_1}\right)^2 + \left(\frac{PE_{Y_2}}{Y_2}\right)^2 \times \left(\frac{Y_1}{Y_2-Y_1}\right)^2 + \left(\frac{PE_T}{T}\right)^2 \tag{29}$$

The power ratio Y_2 is given by

$$Y_2 = \frac{T_0 + T_r}{T_{sa}} \tag{30}$$

where

T_{sa} = system effective noise temperature, defined at the receiver input reference plane, with the radio source outside the antenna beam, °K

If PE_{Y_2} is the probable error of the measurement of Y_2, then

$$\left(\frac{PE_{Y_2}}{Y_2}\right)^2 = \left(\frac{PE_{T_{sa}}}{T_{sa}}\right)^2 + \left(\frac{1}{\tau B}\right) + \left(\frac{\Delta G}{G_0}\right)^2 + (a_1)^2 + [a_2 Y_2\,(\mathrm{dB})]^2 \tag{31}$$

The power ratio Y_1 is given by

$$Y_1 = \frac{T_0 + T_r}{T_{sa} + T'} = \frac{T_0 + T_r}{T_{ss}} \tag{32}$$

where

T' = measured radio source temperature, °K

T_{ss} = system effective noise temperature, defined at the receiver input reference plane, with the antenna on a radio source, °K

The probable error of the measurement of Y_1 is given by

$$\left(\frac{PE_{Y_1}}{Y_1}\right)^2 = \left(\frac{PE_{T_{ss}}}{T_{ss}}\right)^2 + \frac{1}{\tau B} + \left(\frac{\Delta G}{G_0}\right)^2 + (a_1)^2 + [a_2 Y_1\,(\mathrm{dB})]^2 \tag{33}$$

The Y-factor measurement accuracies in terms of known parameters are given by Eqs. (31) and (33). Error terms, such as PE_{T_0} and PE_{T_r}, do not enter these equations because any change in ambient temperature or receiver noise temperature while the Y-factor is being measured will be small and may, therefore, be neglected. In Eq. (31), $PE_{T_{sa}}/T_{sa}$ is also negligibly small during the Y-factor measurement. The error term, $PE_{T_{ss}}/T_{ss}$, arises from an antenna boresight and tracking error on the radio source. This error term was analyzed and an expression found for $PE_{T_{ss}}$ (Ref. 4). Equations (29), (31), and (33) are the

Table 2. Summary of antenna efficiency measurements at stations 11 and 12

Source	Station	$L_0 = 0$ dB		$L_0 = 0.05$ dB		$L_0 = 0.1$ dB	
		η, %	σ, %	η, %	σ, %	η, %	σ, %
Omega	11	48.93	1.63	50.09	1.59	51.28	1.57
	12	54.21	0.87	55.56	1.07	56.94	1.37
Taurus A	11	49.00	0.65	49.82	0.62	50.66	0.61
	12	58.99	0.59	56.81	0.74	57.65	0.92

defining equations for the probable error of the measurement of antenna efficiency. These equations have been programmed in Fortran and the data reduced by computer. It was found that, assuming T is known, the antenna efficiency can be measured with a probable error of 0.007. This error contributes an additional 0.05 dB to the incident power measurement error if antenna efficiency is taken into account.

The total probable error of the determination of antenna efficiency is made up of the measurement probable error previously mentioned, a term which takes into account the uncertainty in the knowledge of the assumed radio source temperature, T, and the bias errors in the antenna gain measurement. The term, which takes into account both bias and the uncertainty in the knowledge of T, was estimated as 0.2 dB. Combining these error terms yields the value 0.40 dB for PE_η.

4. Step-attenuator correction. The precision RF attenuator shown in Fig. 1 consists of both step and variable attenuators. If the step attenuator is changed at any time during the AGC curve calibration, it is necessary to correct for step-attenuator errors. Normal station procedure is to change the step attenuator at predetermined signal generator levels. The steps used were calibrated as a separate experiment. The radiometer system was used as the calibration equipment, and careful attention was given to linearity, signal level, and saturation. The two switching steps normally used at each station were calibrated over a period of several weeks. The data were averaged to yield correction factors SA1 and SA2, which then formed part of the constant station input data. There does not appear to be any advantage in providing for a step attenuator for the AGC calibration, since the variable attenuator has sufficient dynamic range.

E. Measurements

1. System temperature.

a. Theory and measurement. CW power calibrations were carried out over an extended period of time on *Mariner IV*. Because these calibrations were made at two stations, it was important, for comparative purposes, that both stations use the same method of system temperature measurement. Among other constraints on the measurement of system temperature were: (1) the requirement for reliability and repeatability, as the experiments continued over an extended period of time, and (2) the need for a quick and simple method, because of the limited time available during the pretracking routine. Because of these constraints, a Y-factor method was chosen. An ambient load was chosen because it met the requirements of reliability and stability; an ambient load is convenient from an operational point of view, and is sufficiently accurate for these measurements. Switching the maser input between the antenna at zenith and the ambient load yielded the Y-factor, Y_{a0}. Each station measured five Y-factors daily during the pretracking routine and just prior to the CW power calibration. An average system temperature for each station was computed each day from these measurements. This method requires a knowledge of the thermal temperature of the termination. The thermal temperature of the ambient load, T_0, which can easily be determined with sufficient accuracy, was read on a mercury thermometer inserted in a massive copper block surrounding the waveguide termination.

The receiver temperature, T_r (approximately 10°K), was measured with precision cryogenic terminations and was assumed to be constant throughout the experiment. The long-term stability of the receiver noise temperature was better than that of the coaxial cryogenic termination available in the system.

b. Error analysis. System temperature, defined at the receiver input reference flange, was computed from

$$T_s = \frac{T_0 + T_r}{Y_{a0}} \tag{34}$$

An error analysis of this equation has been performed (Ref. 4). If the system's temperature probable error is

PE_{T_s}, then

$$\left(\frac{PE_{T_s}}{T_s}\right)^2 = \left(\frac{PE_{T_0}}{T_0}\right)^2 \left(1 - \frac{T_r}{T_s Y_{a0}}\right)^2 + \left(\frac{PE_{T_r}}{T_r}\right)^2 \left(1 - \frac{T_0}{T_s Y_{a0}}\right)^2 + \left(\frac{PE_{Y_{a0}}}{Y_{a0}}\right)^2 \quad (35)$$

The probable error ratio $PE_{Y_{a0}}/Y_{a0}$, in the Y-factor measurements, is a function of:

(1) The attenuator resetability and linearity constants, a_1 and a_2, defined above.

(2) Receiver gain instability,

$$\left[\frac{1}{\tau B} + \left(\frac{\Delta G}{G_0}\right)^2\right]^{1/2}$$

(3) An error term caused by the measurement scatter on the Y-factors.

The term in item (3) is derived as follows:

If the measured Y-factors are $Y_{a0i\,(\mathrm{dB})}$, $i = 1, \cdots, 5$, then the average Y-factor is

$$\overline{Y}_{a0\,(\mathrm{dB})} = \sum_{i=1}^{N'} \frac{Y_{a0i\,(\mathrm{dB})}}{N'} \quad (36)$$

where

$$N' = 5$$

The probable error of the average Y-factor is

$$PE_{\overline{Y}_{a0\,(\mathrm{dB})}} = \frac{0.6745}{[N'(N'-1)]^{1/2}} \left[\sum_{i=1}^{N'} (\overline{Y}_{a0\,(\mathrm{dB})} - Y_{a0i\,(\mathrm{dB})})^2\right]^{1/2} \quad (37)$$

All the Y-factors in Eqs. (36) and (37) have units of decibels. The error term (item 3) is then given by the probable error ratio derived from Eq. (37):

$$\frac{PE_{y_{a0}}}{y_{a0}} = \left(\frac{\ln 10}{10}\right) \cdot PE_{\overline{Y}_{a0\,(\mathrm{dB})}} \quad (38)$$

where

$$\frac{PE_{y_{a0}}}{y_{a0}}$$

is a ratio and is the required error term (item 3). Therefore, the probable error ratio

$$\frac{PE_{Y_{a0}}}{Y_{a0}}$$

in Eq. (35) is given by

$$\left(\frac{PE_{Y_{a0}}}{Y_{a0}}\right)^2 = a_1^2 + [a_2 \overline{Y}_{a0\,(\mathrm{dB})}]^2 + \left[\frac{1}{\tau B} + \left(\frac{\Delta G}{G_0}\right)^2\right] + \left(\frac{PE_{y_{a0}}}{y_{a0}}\right)^2 \quad (39)$$

If the temperature of the termination is considered variable and written T_1 instead of T_0, then a graph of Eq. (35) may be drawn. This is shown in Fig. 8 where normalized system temperature probable error is drawn as a function of termination temperature for different values of receiver temperature probable error. The following values have been used for the various parameters:

$$\frac{1}{\tau B} = 10^{-5} \qquad \frac{\Delta G}{G_0} = 0.005\,\mathrm{dB}$$

$$a_1 = 0.003\,\mathrm{dB} \qquad a_2 = 0.00354\,\mathrm{dB}$$

The more accurate the evaluation of the receiver temperature, the more accurate will be the system temperature measured by this method. The probable errors in the receiver temperature used in Fig. 8, 1 and 0.2°K, are typical of the present DSN systems and a receiver system evaluated with well-calibrated waveguide terminations, respectively. The importance of the accuracy of the evaluation of receiver temperature diminishes with higher temperature termination standards. The ambient temperature termination for the present experiment appears to be a reasonable choice.

c. Results and discussions. Low maintenance time and low operating cost are the practical advantages that an ambient temperature termination has over a cryogenic termination. The ambient termination also simplifies the problem of determining the equivalent noise temperature of the termination defined at the receiver input reference plane. The use of an ambient termination for routine system temperature measurements does not reduce the importance of a well-calibrated cryogenic termination. The cryogenic termination can be used periodically to re-evaluate the receiver temperature and to perform other measurements, such as absolute antenna temperature measurements.

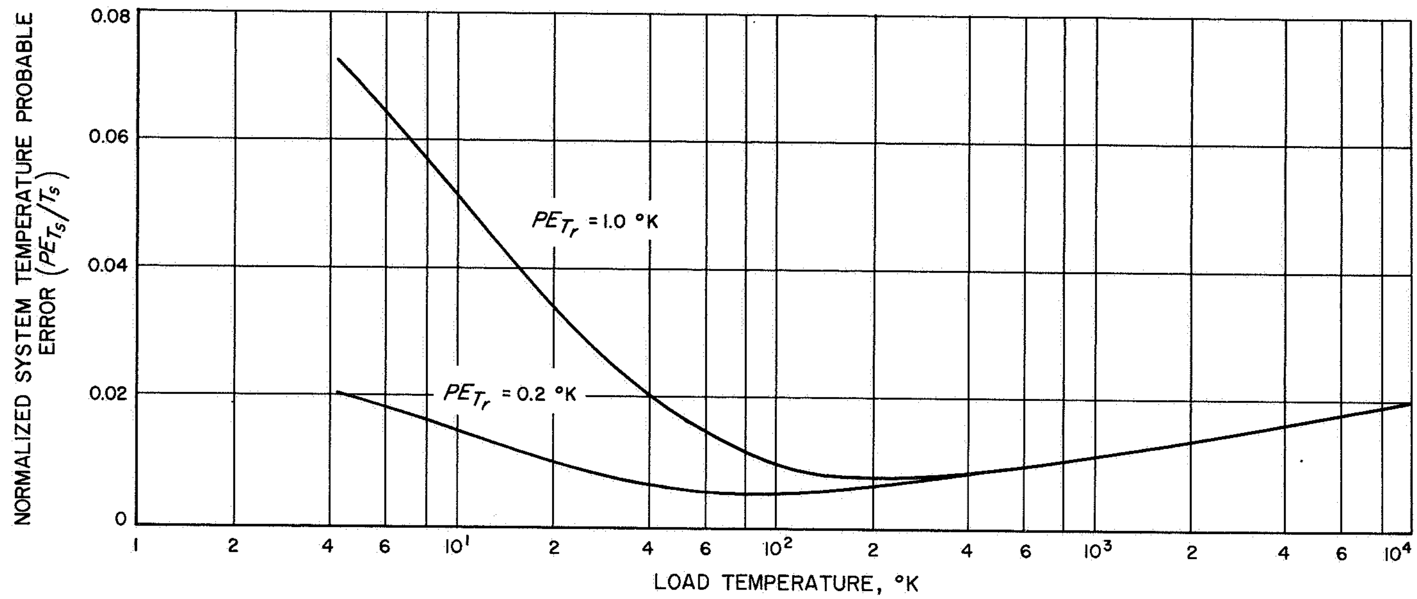

Fig. 8. System temperature probable error vs load temperature

Table 3 presents a summary of system temperature measurements for the Pioneer and Echo stations during the period *Mariner IV* CW power was calibrated by microwave thermal standards. The nominal method refers to the system temperature measurements by the normal station procedures and reported to the Space Flight Operations Facility (SFOF). Figure 9 illustrates system temperature vs time for the two stations. The solid lines connect the data points derived by the ambient termination Y-factor method, and the dotted lines correspond to the nominal station data. The averages from Table 3 are also shown. It should be noted that the system temperature measurements by the ambient termination Y-factor method were made through the narrow-band filter. The resolution would be considerably improved if this narrow-band filter were not used. For example, at the Mars station, where system temperature is measured by an ambient termination Y-factor method without narrow-band filter, the 1σ of one month's data was 0.12°K after adjustment for equalizing the number of data points (Ref. 7). However, even with the narrow-band filter, the 1σ of the measurement data were considerably reduced over that of the nominal data. Furthermore, by comparison, the mean noise temperatures between stations appear more consistent.

Table 3. System temperature measurements at stations 11 and 12

Station	Y-factor method		Nominal DSIF method	
	Average, °K	Standard deviation, °K	Average, °K	Standard deviation, °K
11	44.8	0.55	41.3	0.99
12	43.6	1.18	48.3	2.60

The probable error of the daily system temperature measurements was 0.3°K, a contribution of approximately a 0.03-dB error to the test transmitter calibration.

2. The AGC curves. The calibration power ratio Y-factors were taken by switching the test transmitter on and off. These measurements were performed daily at five separate power levels from −110 to −130 dBmW. These ratios were used with Eq. (7) to obtain calibrated levels of the test transmitters. The test transmitter power level for these points was chosen so that it covered as wide a power range as possible. The calibration range was limited by receiver nonlinearity at high-power levels and loss of signal in the noise at low-power levels. Linearity over the calibration range was carefully checked at each station (Ref. 8).

The power range covered by the nominal AGC curve was normally −110 dBmW down to receiver threshold. Figure 10 shows calibrated and nominal AGC curves for the Pioneer station for July 16, 1965. The average of the individual differences between the calibrated and nominal CW powers yields the correction factor for the calibrated spacecraft power. A statistical second-order curve was fitted to each day's nominal AGC curve data by a least-squares computer method. The constants that define

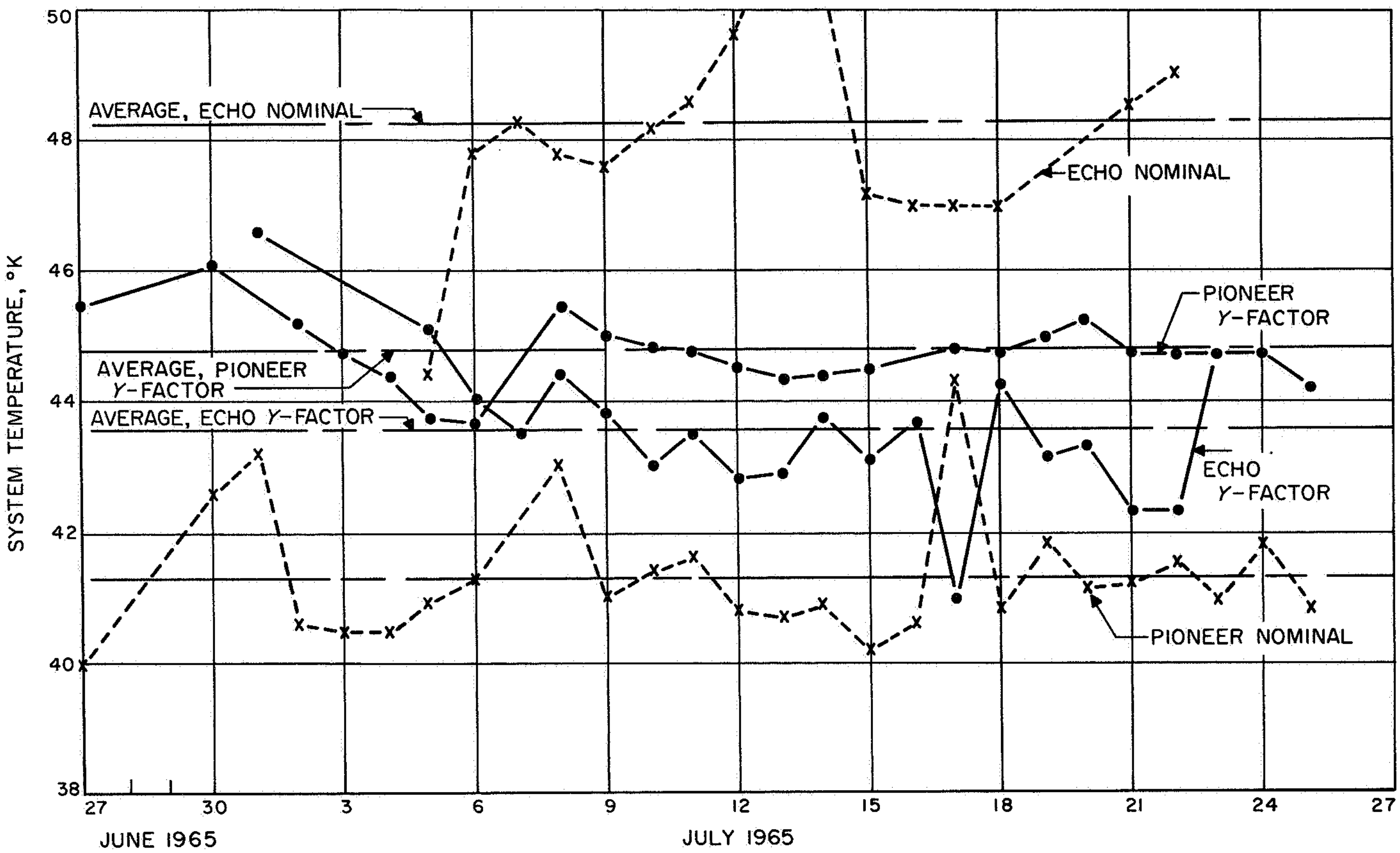

Fig. 9. System temperature measurements at the Pioneer and Echo stations

this curve, and their probable errors, were computed each day and used in the data reduction. The probable error caused by measurement scatter in the AGC curve was typically 0.05 dB. This curve, with the spacecraft AGC voltage, yielded the required power levels.

The computer technique virtually eliminates the error normally caused by the graphical conversion of receiver AGC voltage to spacecraft power. The primary error in extrapolating the correction factor to the spacecraft AGC reading is dependent on the test transmitter attenuator, and is approximated by

$$b\left[10\log_{10}\left(\frac{P^*_{si}}{P_{si}}\right)\right]$$

where b is the test transmitter attenuator nonlinearity. The multiplying factor is the ratio, converted to decibels, of test transmitter input signal power defined at the receiver input reference plane to the spacecraft signal power defined at the receiver input reference plane. This error was typically 0.2 dB and contributed directly to the error of the spacecraft-calibrated power.

3. Atmospheric attenuation. To compare the calibrated power levels (normalized for 100% antenna efficiency) between stations, it is also necessary to account for atmospheric attenuation, which is a function of zenith angle. The relationship with a flat earth approximation is

$$P'_{si} = P''_{si}\,(L_0)^{-\sec z} \tag{40}$$

where P'_{si} and P''_{si} are defined in Eqs. (8) and (9). The zenith angle and receiver AGC voltages are recorded simultaneously.

a. Error analysis. The analysis of Eq. (40) yields the additional uncertainty caused by the atmospheric attenuation correction:

$$(PE_{P''_{si}})^2 = (PE_{P'_{si}})^2\left(\frac{\partial P''_{si}}{\partial P'_{si}}\right)^2 + (PE_{L_0})^2\left(\frac{\partial P''_{si}}{\partial L_0}\right)^2 + (PE_{\sec z})^2\left(\frac{\partial P''_{si}}{\partial \sec z}\right)^2 \tag{41}$$

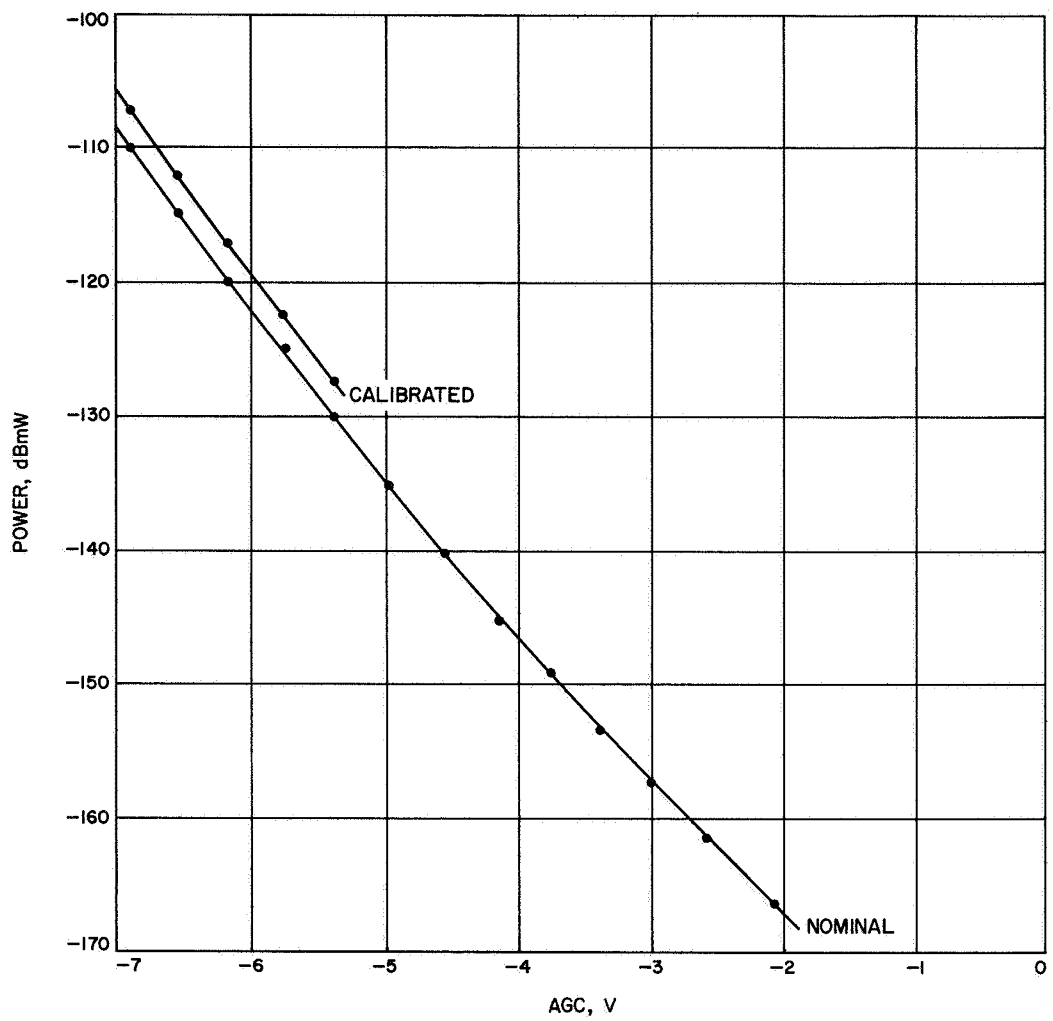

Fig. 10. Nominal and calibrated AGC curves for the Pioneer station, July 14, 1965

Equation (41) may be written as:

$$\left(\frac{PE_{P''_{si}}}{P''_{si}}\right)^2 = \left(\frac{PE_{P'_{si}}}{P'_{si}}\right)^2 + \left(\frac{PE_{L_0}}{L_0}\right)^2 \cdot (\sec z)^2 \qquad (42)$$

where the term

$$(PE_{\sec z})\left(\frac{\partial P''_{si}}{\partial \sec z}\right)$$

has been ignored because the inaccuracy associated with the measurement of zenith angle was generally negligible compared with the inaccuracies associated with P'_{si} and L_0.

Therefore, the additional error of the atmospheric correction is

$$\left(\frac{PE_{L_0}}{L_0}\right) \cdot \sec z$$

which is less than 0.1 dB for spacecraft zenith angles <70 deg, if PE_{L_0} is taken as 0.01 dB.

IV. Data Reduction

A general description of the data reduction method which was automated with computer techniques is presented in this section. The computer program is listed in Appendix A and discussed in Appendix B.

A. Methods of Reduction

1. Computer input. The computer input consists of station constants and preliminary information, such as date, time, ambient temperature, and measurement data.

2. System temperature. The system temperature is computed from Eqs. (34) and (36), and system temperature probable error is computed from Eqs. (35) and (39).

3. The calibrated AGC curve. The computed value of system temperature is used in Eq. (7) to determine the five calibrated test transmitter power levels which define the calibrated AGC curve.

4. The correction factor. The nominal and calibrated test transmitter power levels yield the correction factor COR, which is the average difference between these levels. The variance of the scatter of the values of COR is computed.

5. The nominal AGC curve. To compute probable errors correctly from a curve fitted to the nominal AGC data, it is convenient to translate the Y-axis (power axis) to the AGC voltage at which power is to be calibrated. If only one reading of receiver AGC voltage on the spacecraft is obtained in a day, then the Y-axis is translated to that point. If several AGC voltage readings on the spacecraft are obtained, then the Y-axis is translated to the average of these voltages. AGC voltage data on the spacecraft are designated GNAGC. The program determines the number NN of GNAGC data points and computes their average which is designated A3. After the transformation of the Y-axis to the appropriate point, the program calls the subroutine FITA2. This subroutine fits the best second-order curve by a least-squares method to the nominal AGC data from $i = 6$ to $i = N$, where N is the total number of nominal AGC curve data points. The first five data points are the high-power calibration points. These points are ignored by the subroutine FITA2 because it is desirable to curve-fit in the region of the spacecraft AGC readings, which correspond to low-power data down to receiver threshold.

The subroutine FITA2 also determines the constants A_1, B_1, and C_1 of the best-fit curve

$$Y = A_1 + B_1 x + C_1 x^2 \tag{43}$$

and the probable errors of A_1, B_1, C_1, and the individual data points Y_1.

6. Nominal AGC curve deviations. The deviation of each nominal AGC data point, from $i = 6$ to $i = N$, from the corresponding voltage point on the computed curve, Eq. (43), is computed and printed in the output.

7. Nominal and calibrated spacecraft power levels. The nominal value of received spacecraft power is given by the constant A_1 in Eq. (43), because the Y-axis was transformed to the point on the calibrated value of received spacecraft power P_{si}, and is found by applying the correction factor COR, to the nominal power A_1.

8. Probable error of the calibration of the test transmitter. The probable error of the calibration of the test transmitter level (microwave thermal standards method) is computed by Eq. (11). This does not include the error caused by the scatter of the individual correction factors. When these individual correction factors are averaged, they yield the term COR. When the scatter term PE_{COR} is added to Eq. (11), the result is the final calibration probable error of the test transmitter level. This is defined E5 as a ratio, or as EC5 in decibels.

$$(\mathrm{E5})^2 = \left(\frac{PE_Y}{Y}\right)^2 \left[1 + \frac{k\,T_s\,B}{P^*_{si}\,g\,(f_s)}\right]^2 + \left(\frac{PE_{T_s}}{T_s}\right)^2 + \left(\frac{PE_B}{B}^2\right) + \left[\frac{PE_{g\,(f_s)}}{g\,(f_s)}\right]^2 + \left(\frac{PE_\alpha}{\alpha}\right)^2 + \left(\frac{PE_{COR}}{COR}\right)^2 \tag{44}$$

The term PE_{COR}/COR is given by Eqs. (58) and (59) in Appendix B.

9. Probable error of the nominal spacecraft power. The nominal AGC curve is given by Eq. (43):

$$Y = A_1 + B_1 x + C_1 x^2$$

Nominal spacecraft power is given by this equation when $x = 0$, i.e.,

$$\text{Nominal Spacecraft Power} = A_1 \tag{45}$$

To determine the probable error of the nominal spacecraft power, an error analysis is performed on Eq. (43) as follows:

$$(\mathrm{E10})^2 = (PE_{A_1})^2 + (PE_{B_1})^2 x^2 + (PE_{C_1})^2 x^4 + (PE_x)^2 (B_1 + 2C_1 x)^2 \tag{46}$$

where E10 is the probable error of the nominal spacecraft power in decibels. The value of E10 corresponding to a nominal spacecraft power equal to A_1 is given by Eq. (46) when $x = 0$.

Thus,

$$(\mathrm{E10})^2 = (PE_{A_1})^2 + (PE_x)^2 (B_1)^2 \tag{47}$$

PE_{A_1} and B_1 are determined from the subroutine FITA2. PE_x is computed as follows.

In the original system of coordinates,

$$GNAGC_i, i = 1 \cdots NN$$

are the receiver AGC voltage data on the spacecraft. The power axis was transformed to the point

$$A_3 = \frac{1}{NN}\sum_{i=1}^{NN} GNAGC_i \tag{48}$$

Then,

$$(PE_{A_3})^2 = \frac{(0.6745)^2}{NN-1}\sum_{i}^{NN}(A_3 - GNAGC_i)^2 \tag{49}$$

PE_{A_3} is substituted for PE_x in Eq. (47).

Some other error terms must be added to Eq. (47) before it adequately describes the probable error of the nominal spacecraft power. These additional terms are:

a_3 = Receiving system nonlinearity, RF to IF.

a_4 = Nonlinearity and calibration of the variable attenuator in the test transmitter.

a_5 = Calibration of the step attenuator in the test transmitter.

a_6 = AGC voltage indicator jitter.

a_7 = Antenna-to-spacecraft pointing error.

PE_{TTC} = Probable error of the test transmitter calibration (nominal method).

These terms are summarized by the expression:

$$\left[\sum_{i=3}^{7}(a_i)^2\right] + (PE_{TTC})^2 = (PE_{se})^2 + (PE_{TTC})^2$$

where PE_{se} = the effective probable error ratio arising from the summation of the error terms a_3 through a_7.

The complete defining equation of the probable error of the nominal spacecraft power, defined at the receiver reference flange, is

$$(\mathrm{E10})^2 = (PE_{A_1})^2 + (PE_{A_3})^2 \cdot (B_1)^2 + (PE_{se})^2 + (PE_{TTC})^2 \tag{50}$$

which may be written as

$$(\mathrm{E10})^2 = (\mathrm{E7})^2 + (PE_{TTC})^2 \tag{51}$$

where

$$(\mathrm{E7})^2 = (PE_{A_1})^2 + (PE_{A_3})^2 \cdot (B_1)^2 + (PE_{se})^2 \tag{52}$$

The term E7 represents the summation of all error contributions common to both the microwave thermal standards method and the nominal method.

10. Probable error of the calibrated spacecraft power. The probable error of the calibrated spacecraft power is given by summing the common error contributions, E7, and the errors caused by the calibration of the test transmitter by the microwave thermal standards method, E5. The probable error of the calibrated spacecraft power defined at the receiver reference flange is then

$$(\mathrm{E8})^2 = (\mathrm{E7})^2 + (\mathrm{E5})^2 \tag{53}$$

11. Spacecraft power normalized for 100% antenna efficiency. The calibrated spacecraft power is normalized for 100% antenna efficiency. Equation (8) is the normalizing equation:

$$P'_{si} = \frac{P_{si}}{\eta}$$

where

P'_{si} = power incident on the antenna

P_{si} = calibrated spacecraft power defined at the receiver input reference plane

η = antenna efficiency defined at the receiver input reference plane

12. Spacecraft power corrected for atmospheric loss. The calibrated spacecraft signal power that would be incident on the antenna with atmospheric loss removed is given by Eq. (9) as follows:

$$P''_{si} = (P'_{si})\,(L_0)^{\sec z}$$

where

L_0 = atmospheric loss at zenith

z = zenith angle

13. Incident power. With NN values of receiver AGC voltage on the spacecraft in a day, the data reduction program computes NN values of: (1) nominal spacecraft power; (2) calibrated spacecraft power; (3) calibrated and normalized spacecraft power; and (4) spacecraft power, calibrated, normalized, and corrected for atmospheric loss.

The requirement now is to determine the best estimate of received spacecraft power. The receiver AGC voltages on the spacecraft, GNAGC, in one track, will vary for several reasons. For example, receiver gain may change during the track, zenith angle (atmospheric attenuation) will change, spacecraft orientation may change, etc. The longer the time delay between the evaluation of the correction factor, COR, during the station pretracking routine and the measurement of the GNAGC voltages on the spacecraft, the less accurate the final result. This problem can be partially avoided by taking atmospheric loss into account and by fitting a curve to the observed data and extrapolating to zero normalized time, i.e., determining a value for received spacecraft power at the calibration time. A straight line

$$Y_5 = A_5 + B_5 x \tag{54}$$

is fitted to these data by a least-squares method with a weighting factor w, where

Y_5 = incident power

x = normalized time of measurement

A_5, B_5 = straight-line constants from the statistical analysis

This line is extrapolated to the calibration time and the best estimate of received spacecraft power is given by A_5.

The defining equations are sufficiently general so that it is immaterial whether it is a precalibration or a postcalibration.

14. Probable error of the incident power. From Eq. (9), which corrects received power for atmospheric loss,

$$\left(\frac{PE_{P''_{si}}}{P''_{si}}\right)^2 = \left(\frac{PE_{P'_{si}}}{P'_{si}}\right)^2 + \left(\frac{PE_{L_0}}{L_0}\right) \cdot (\sec z)^2 + (PE_{\sec z})^2 \cdot \left(\frac{\partial P''_{si}}{\partial \sec z}\right)^2$$

The inaccuracy in the measurement of zenith angle is generally negligible compared with the inaccuracies associated with the terms L_0 and P'_{si}. The term containing $PE_{\sec z}$ is therefore ignored, and the error equation is written

$$\left(\frac{PE_{P''_{si}}}{P''_{si}}\right)^2 = \left(\frac{PE_{P'_{si}}}{P'_{si}}\right)^2 + \left(\frac{PE_{L_0}}{L_0}\right)^2 \cdot (\sec z)^2 \tag{55}$$

A probable error is associated with each of the NN computed data points for the first-order analysis. This probable error is made up of (1) a part which is a function of zenith angle and is a measure of the scatter of the data about the line $Y_5 = A_5 + B_5 x$, and (2) a part which is not a function of zenith angle but is associated with the uncertainty in the determination of COR, the power correction factor, and the antenna normalization. The only term in Eq. (55) that is a function of zenith angle is

$$\left(\frac{PE_{L_0}}{L_0}\right) (\sec z)$$

This term may, therefore, be used as a weighting factor in the straight-line analysis to reduce the effect of those less accurate measurements taken at high zenith angles. Hence, the weighting factor is given by

$$w = \left[\left(\frac{PE_{L_0}}{L_0}\right) \sec z\right]^{-2} \tag{56}$$

The straight-line analysis (subroutine FIT1) yields the constants A_5, B_5, and the probable error of A_5, PE_{A_5}. If insufficient data points are available to perform a statistical first-order analysis ($NN \leqq 2$), the first data point is defined as A_5 and its probable error as $[(PE_{L_0}/L_0) \sec z]$.

The term E9 is the probable error of the incident power, and is given by the sum of the following terms:

(1) Probable error of the calibrated spacecraft power level E8 (Eq. 53).

(2) Probable error of the incident power caused by the scatter of the data points about the straight line, PE_{A_5}.

(3) Probable error of the antenna efficiency PE_η, given by Eqs. (29), (31), and (33).

(4) The above three equations define PE_η with the assumption that T, the assumed radio source temperature, is exact. Therefore, a term that takes account of the uncertainty in the knowledge of T must be added.

(5) Bias errors in the antenna gain measurement.

Hence,

$$(\mathrm{E9})^2 = (\mathrm{E8})^2 + \left(\frac{PE_{A_5}}{A_5}\right)^2 + \left(\frac{PE_\eta}{\eta}\right)^2 + 0.0085 \tag{57}$$

where 0.0085 is a squared ratio and represents the bias errors in the antenna gain measurement, estimated as 0.4 dB.

15. Incident power density. The spacecraft incident power, P''_{si}, is defined as A_5. The incident power density is then computed in terms of antenna aperture A, from P''_{si}/A. Received power density should be calculated because it enables comparisons between different stations which track the same spacecraft, but which have different antenna diameters.

B. Discussion

A block diagram of the error analysis is shown in Fig. 11. The diagram is divided into three sections: (1) the first section shows the important errors arising in the microwave thermal standards method, (2) the middle section shows the errors common to both methods, and (3) the third section shows the errors arising from the nominal calibration method. The diagram, as a whole, shows the interrelationship of the various errors and summarizes the overall error analysis.

In Fig. 11, the errors are shown in the rectangular blocks. Each block has a numerical value of the errors described in that block. These values are either average computed errors in decibels, or estimated errors in decibels. Thus, EC2, the probable error of the computed system temperature (see Nomenclature and Subsection

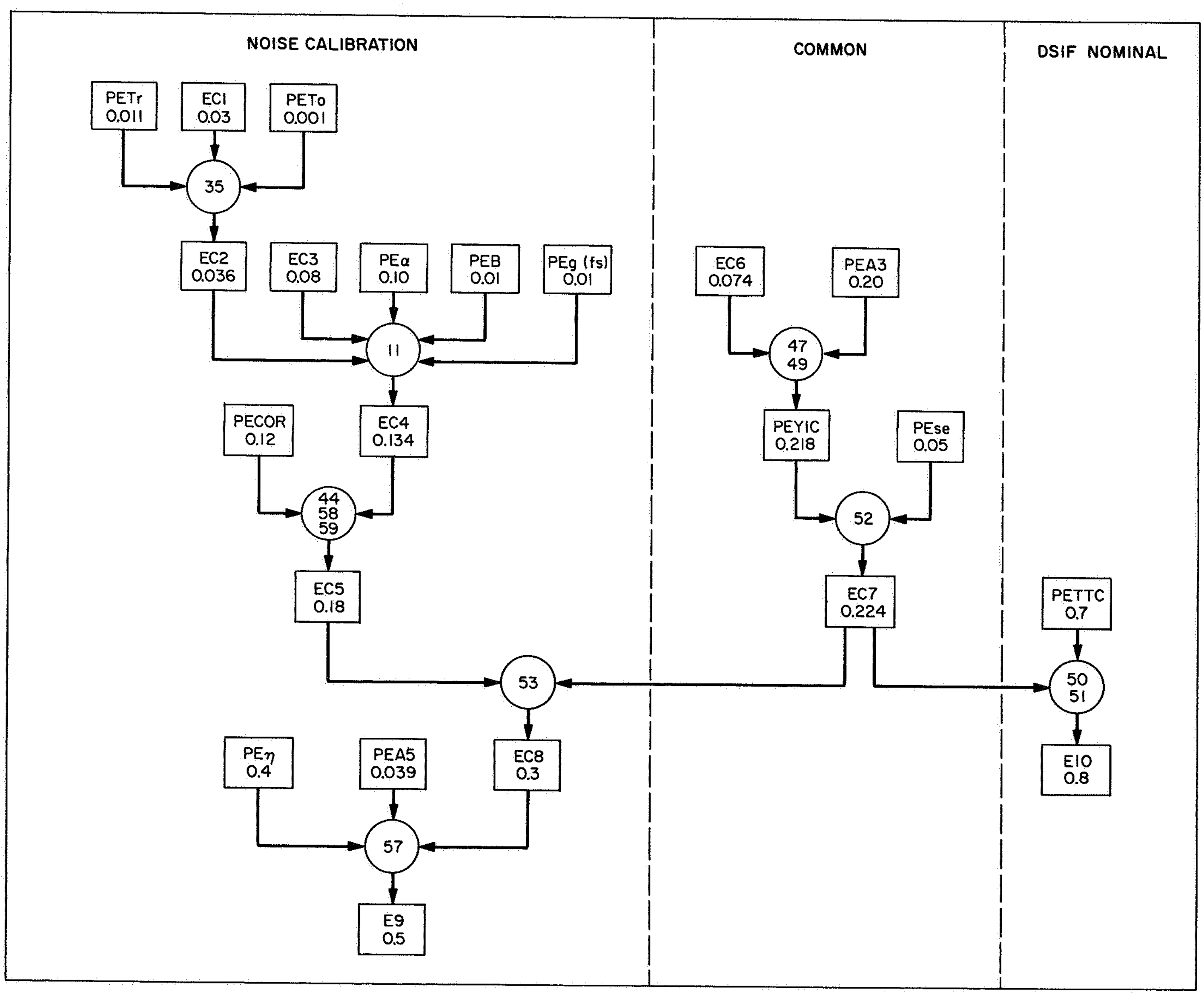

Fig. 11. Block diagram of error analysis

III-E-1), has an average computed value of 0.036 dB. The probable error of the system temperature, EC2, is computed by Eq. (35) which combines the errors caused by the uncertainty in the measurement of receiver temperature PE_{T_r}, the uncertainty in the determination of the ambient temperature PE_{T_0}, and the measurement errors associated with the system temperature Y-factors. These latter errors are designated EC1. Equation (35) combines these errors with multiplying factors on PE_{T_r} and PE_{T_0}. The magnitude of the error in decibels, as shown in each of the blocks, includes the effect of any multiplying factor which may be associated with the error term in a combining equation.

Similarly, Eq. (11) combines five error terms shown in Fig. 11 to yield EC4. Then, with the addition of a term which takes into account the measurement scatter of data points, the probable error of the calibration of the test transmitter by the microwave thermal standards method is found. This is designated EC5.

The sum of the errors common to both methods is EC7. As shown in Fig. 11, this sum is combined with EC5 in Eq. (53) to yield EC8, the probable error of the calibrated spacecraft power by the microwave thermal standards method. This sum is combined with PE_{TTC} in Eqs. (50) and (51) to yield the probable error of the spacecraft power by the nominal method. These errors are 0.3 and 0.8 dB, respectively.

The probable error of the incident power, E9, is computed by Eq. (57), which combines the three error terms shown in the figure. The average incident power probable error is 0.37 dB.

V. Results and Conclusions

The data reduction, including the error analysis, is computed for each day's tracking at each station. The computer printout for the Pioneer station for the day of encounter (July 14, 1965) is shown in Fig. 12. Figure 13 shows the computer printout for the Mars station (DSS 14, 210-ft antenna) for May 21, 1966. Input data, consisting of station constants and measurements, are printed out on the upper portion, while computed outputs are listed below. The Pioneer and Echo stations measured only one spacecraft CW power per day and, therefore, only one AGC voltage data point is shown in Fig. 12 under SIGNAL AGC. On May 21, 1966, the Mars station measured 21 signal AGC data points, and a first-order statistical curve was computed as described in Subsection IV-A-15. The constants of this line show that the measured incident power at the time of calibration was -168 dBmW (omnidirectional spacecraft antenna), and that the slope of the line over almost 7 h 30 min of tracking was 0.091 dB/h. The range of *Mariner IV* at the time of calibration was approximately 317.43×10^6 km, or 197.24×10^6 mi. Figures 12 and 13 also show the measured incident power converted to a power density (dBmW per m^2 of antenna aperture). Figure 13 shows a received power density of -203.172 dBmW/m^2 corresponding to a measured incident power of -168.1 dBmW.

Figure 12 shows that the power correction factor at the Pioneer station is positive. However, the power correction factor at the Echo station is negative. This is reflected in Fig. 14, which shows second-order statistical curves fitted by a least-squares method to the nominal, calibrated, and incident power levels as a function of the year and day, at the Pioneer and Echo stations. The data are centered about the day of Mars encounter, July 14, 1965. Data points with deviations greater than 2 from the curves (three from Pioneer, two from Echo) have been discarded. The difference between the nominal power curves for the Pioneer and Echo stations is greater than expected from the error analysis, probably because of the exceptionally high errors of the test transmitter nominal calibrations. This is indicated by the improved agreement of the calibrated powers between stations. The incident power curves differ at encounter by 0.17 dB. The average incident power level for the two stations is, at encounter, -154.2 dBmW. The portion of the probable error of the calibrated power curves caused by the statistical measurement errors was 0.12 and 0.13 dB at the Pioneer and Echo stations, respectively. If the measurements at the two stations are considered independent, the probable error of the overall power measurement defined at the receiver input, accounting for bias and statistical measurement errors, was 0.2 dB. The theoretically predicted[1] incident power level normalized for 100% antenna efficiency was -153.1 dBmW. The difference of 1.1 dB between the measured and predicted power at encounter is within the error tolerances (Ref. 9).

It was shown that the calibration of the diode detector to the relative noise and CW power sensitivity adds considerable complexity to the measurements. It is recommended that future calibration systems utilize a detector system immuned to errors from the signal form factor.

[1]Private communication, J. Hunter, Jet Propulsion Laboratory, Feb., 1966.

CW POWER CALIBRATION

MARINER 4 SPACECRAFT RECEIVED POWER CALIBRATED WITH MICROWAVE NOISE STANDARDS

STATION 11   DATE 7-14-1965   DAY NO. 195   TIME 2000

AIL-CAL REFERENCE 10.00 DB   AMB-LOAD TEMP. 23.00 C   ANT. EFF. 49.96 PERCENT

GFSK= -198.39 DB   BWR= 11454.800 CPS   ALPHA= .410 DB   TS= 44.42 DEGREES

DATA POINT	AGC VOLTS	LEVEL SET DBM	DEV. DB	AIL ATT DB	CAL-POWER DBM	CORR. DB
1	-6.87	-110.00		43.86	-107.05	2.94
2	-6.52	-115.00		38.91	-112.00	2.99
3	-6.16	-120.00		33.92	-117.01	2.98
4	-5.75	-125.00		28.58	-122.39	2.60
5	-5.37	-130.00		23.81	-127.28	2.71
6	-4.96	-135.23	0.00			
7	-4.54	-140.23	.06			
8	-4.13	-145.23	-.16			
9	-3.75	-149.23	.09			
10	-3.37	-153.37	.06			
11	-3.00	-157.37	-.07			
12	-2.59	-161.37	.03			
13	-2.07	-166.37	0.00			

DATA POINT	SIGNAL AGC	NORMALIZED TIME	NOMINAL DBM	ZENITH ANGLE	AIL-ATT AMB	AIL-ATT SKY
1	-2.68	0.00	-160.51	77.45	18.38	10.00
2					18.40	10.00
3					18.40	10.00
4					18.37	10.00
5					18.40	10.00

NOMINAL AGC CURVE				RECEIVED SIGNAL SLOPE			
A=	-160.51464	PE=	.03386	A=	-154.42223	PE=	.04604
B=	-9.90177	PE=	.05864	B=	0.00000	PE=	0.00000
C=	.52095	PE=	.03093			PEY=	0.00000
		PEY=	.06907				

CORRECTION FACTOR= 2.848 DB

ERROR CONTRIBUTIONS		*****	RECEIVED POWER
EC1=	.004265		NOMINAL=-160.514 DBM
EC2=	.036677		PE= .731 DB
EC3=	.086267		CALIBRATED=-157.666 DBM
EC4=	.138124		PE= .280 DB
EC5=	.183014		INCIDENT POWER=-154.422 DBM
EC7=	.209286		PE= .370 DB
			POWER DENSITY=-181.641 DBM/SQ METER

Fig. 12. Computer printout, Pioneer station, July 14, 1965

CW POWER CALIBRATION

KAMRATH / NIXON MARINER 4 CLEAR WEATHER WINDY 2297 KMC POST-CAL

STATION 14 DATE 5-21-1966 DAY NO. 142 TIME 103

AIL-CAL REFERENCE -3.21 DB AMB-LOAD TEMP. 29.74 C ANT. EFF. 65.00 PERCENT

GFSK= -198.39 DB BWR= 9477.293 CPS ALPHA=0.000 DB TS= 27.10 DEGREES

DATA POINT	AGC VOLTS	LEVEL SET DBM	DEV. DB	AIL ATT DB	CAL-POWER DBM	CORR. DB
1	-4.62	-110.00		29.79	-111.29	-1.29
2	-4.49	-115.00		25.16	-115.92	-.92
3	-4.33	-120.00		19.97	-121.13	-1.13
4	-4.14	-125.00		14.94	-126.20	-1.20
5	-3.94	-130.00		10.15	-131.13	-1.13
6	-3.71	-135.00	.02			
7	-2.07	-160.00	-.18			
8	-1.58	-165.00	.11			
9	-1.37	-167.00	.01			
10	-1.24	-168.00	.11			
11	-1.13	-169.00	.01			
12	-1.00	-170.00	0.00			
13	-.83	-171.00	.13			
14	-.73	-172.00	-.21			
15	-.52	-173.00	-.05			
16	-.29	-174.00	.03			

DATA POINT	SIGNAL AGC	NORMALIZED TIME	NOMINAL DBM	ZENITH ANGLE	AIL-ATT AMB	AIL-ATT SKY
1	-.99	-8.71	-170.00	44.41	7.41	-3.22
2	-1.08	-8.04	-169.39	36.45	7.39	-3.22
3	-1.10	-7.21	-169.22	27.07	7.43	-3.24
4	-1.05	-6.88	-169.58	23.69	7.43	-3.20
5	-1.08	-6.71	-169.39	22.13	7.40	-3.21
6	-1.12	-6.38	-169.08	19.38		
7	-1.08	-6.04	-169.38	17.33		
8	-1.02	-5.71	-169.81	16.25		
9	-1.05	-5.38	-169.57	16.33		
10	-1.04	-5.21	-169.69	16.81		
11	-1.09	-4.88	-169.32	18.53		
12	-1.05	-4.54	-169.55	21.05		
13	-1.11	-3.88	-169.16	27.54		
14	-1.16	-3.71	-168.77	29.35		
15	-1.11	-3.38	-169.12	33.09		
16	-1.09	-3.21	-169.30	35.02		
17	-1.16	-2.71	-168.78	40.93		
18	-1.13	-2.38	-168.97	44.94		
19	-1.08	-1.88	-169.37	51.02		
20	-1.12	-1.54	-169.08	55.09		
21	-1.11	-1.38	-169.10	57.13		

NOMINAL AGC CURVE

A=-169.32436 PE= .02896
B= -7.58748 PE= .05650
C= 2.08149 PE= .02611
PEY= .08586

RECEIVED SIGNAL SLOPE

A=-168.09696 PE= .11568
B= .09089 PE= .02138
PEY= .17478

CORRECTION FACTOR= -1.140 DB

ERROR CONTRIBUTIONS *****

EC1= .007388
EC2= .043651
EC3= .084220
EC4= .138886
EC5= .166245
EC7= .221971

RECEIVED POWER

NOMINAL=-169.324 DBM
PE= .734 DB
CALIBRATED=-170.464 DBM
PE= .278 DB
INCIDENT POWER=-168.096 DBM
PE= .383 DB
POWER DENSITY=-203.172 DBM/SQ METER

Fig. 13. Computer printout, Mars station, May 21, 1966

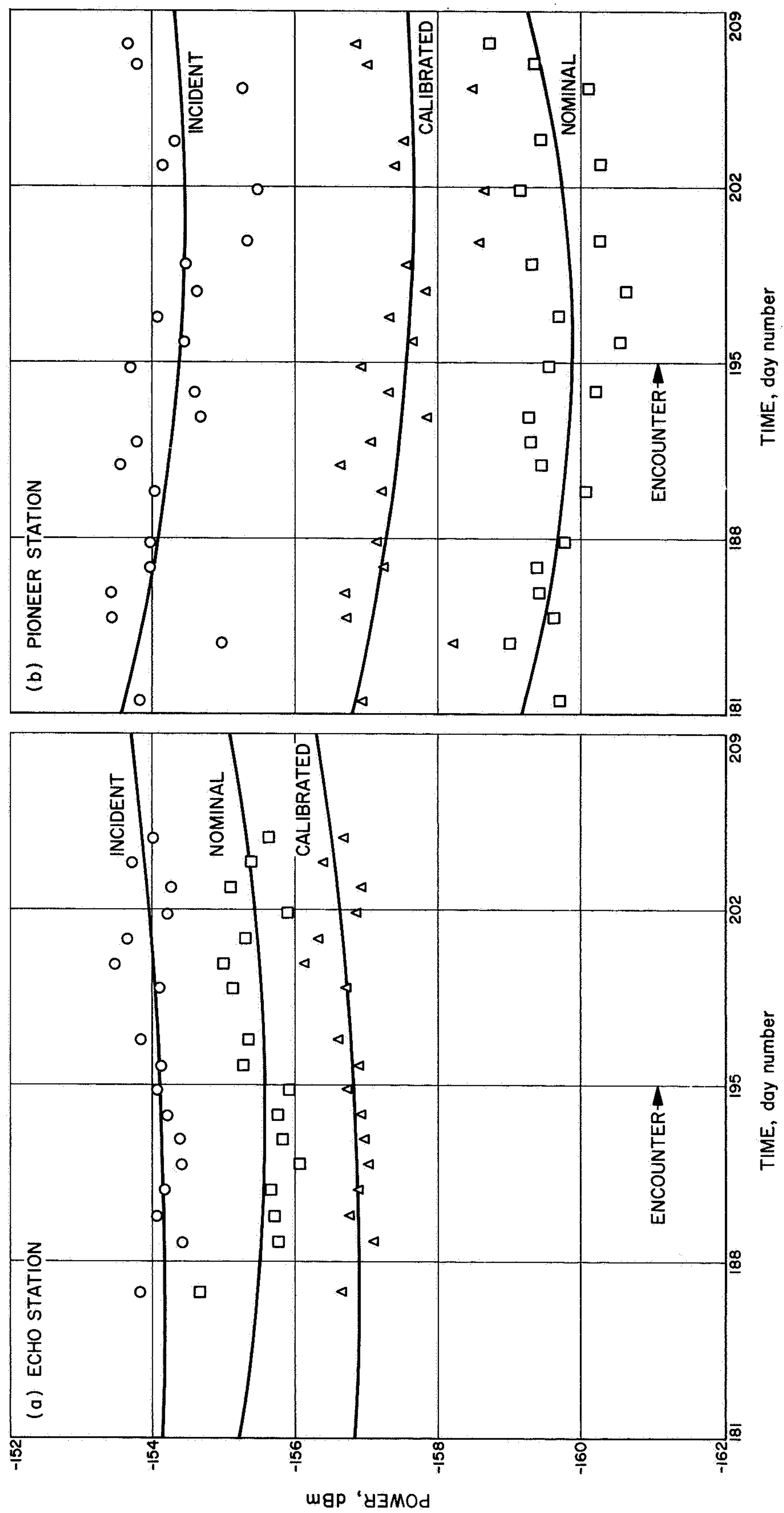

Fig. 14. CW signal level measurements

Appendix A
The Computer Program

```
C                   CW POWER CORRECTION   M.S.REID/D.L.NIXON  5/27/66
      DIMENSION  AGC(25),PSN(25),YDB(5),ATT(5),ERR(25),
     1 PSY(5),YE(5),YO(5),        GNAGC(25),TIME(25),
     2TITLE(20),W(25),DEC(25),HA(25),ADBC(25), PEPP(25),Y2C(25),Z(25)
      ALOGF(XXX)=LOGF(XXX)
      XLO=1.011579
      D=.0174532925199
      PI=3.141592653589793
      CONST1= .230258509299
      CONST2= 4.34294481903
      CONST3= .47717E-06
      CONST4= .6626E-06
      CONST5= .1E-04
      CONST6= .25E-05
      ZZ=0.0
      BK=-198.60
      DO 47 I=1,25
   47 W(I)=1.0
   39 READ 42,TITLE
      READ 10,ITON,MONTH,NDAY,NYEAR,DAYN,H,FM,TO
   48 READ 45,EFF,TR,GFS ,BWR,ALPHA,SA1,SA2,SIZE,PHI
      READ 37,(YO(I),I=1,5)
      READ 37,(YE(I),I=1,5)
      READ 45,YA
      DO 40 I=1,5
   40 READ 45,AGC(I),PSN(I),ATT(I)
      I=5
   41 I=I+1
      READ 45,AGC(I),PSN(I)
      IF (AGC(I)-99.)41,41,4
    4 N=I-1
C
C     CONVERT TIME TO FRACTIONAL DAYS AND NORMALIZE
C     TO CALIBRATION TIME
C
      TUM= DAYN +H/24.0 + FM/1440.
      NYYN=DAYN
      NH=(H*100.)+FM
      I=0
   53 I=I+1
      READ 54,IDAY,HRS,FMIN,GNAGC(I),HA(I),DEC(I)
      IF (IDAY-999)1,1,2
    1 DAY=IDAY
      TIME(I)=(DAY+HRS/24.0+FMIN/1440.0)-TUM
      IF (ABSF(TIME(I))-1.0) 53,55,55
   55 TUM=TIME(I)*24.0
      TYPE 52,TUM
      PAUSE
      GO TO 39
    2 NN=I-1
C
C     COMPUTE SYSTEM TEMPERATURE AND PROBABLE ERRORS
C
      YDBT=ZZ
      DO 56 I=1,5
   56 YDBT=YO(I)-YE(I)+YDBT
      YDBT=YDBT/5.0
      DUM=ZZ
      DO 57 I=1,5
   57 DUM=(YDBT-(YO(I)-YE(I)))**2+DUM
      PEYIT=.6745*(SQRTF(DUM/4.0))
```

```
      PEYDBT=PEYIT/SQRTF(5.0)
      YRT=10.0**(YDBT/10.0)
      E1=PEYDBT*CONST1
      TS=(273.16+TR+TO)/YRT
      TK=TO+273.16
      E2=SQRTF(((.1/TK)**2)*(1.0-TR/(TS*YRT))**2+((1.0/TR)**2)*
     A(1.0-TK/(TS*YRT))**2+(E1**2)+CONST3+CONST4*(YDBT**2)+CONST5
     B   +CONST6)
C
C     CALIBRATION OF TEST TRANSMITTER SIGNAL GENERATOR SIGNAL LEVEL
C
      BWL=CONST2*(ALOGF(BWR))
      T=CONST2*(ALOGF(TS))
      GFSK=BK-GFS
      TGB=T+GFSK+BWL
      YDBAV=ZZ
      DO 23 I=1,5
      YDB(I)=ATT(I)-YA
      YR=10.0**(YDB(I)/10.0)
      Y1DB=CONST2*(ALOGF(YR -1.0))
      YDBAV=YDBAV+YDB(I)
      PSY(I)=Y1DB+ALPHA+TGB
   23 ERR(I)=PSY(I)-PSN(I)
      YDBAV=YDBAV/5.0
      YRAV=10.0**(YDBAV/10.0)
C
C     STEP ATTENUATOR CORRECTION
C
      DO 24 I=1,N
      IF (PSN(I)+130.)16,24,24
   16 IF(PSN(I)+150.0)18,17,17
   17 PSN(I)=PSN(I)+SA1
      GO TO 24
   18 PSN (I)=PSN(I)+SA2
   24 CONTINUE
C
C     CURVE FIT - NOMINAL, CALIBRATED, RECIEVED SPACECRAFT AGC VOLTAGE
C
      AVG=ZZ
      DO 20 I=1,5
   20 AVG=(PSY(I)-PSN(I))+AVG
      COR=AVG/5.0
      DUM=ZZ
      DO 68 I=1,5
   68 DUM=DUM+(COR-(PSY(I)-PSN(I)))**2
      PEA2=.6745*(SQRTF(DUM/4.0))
      A3=ZZ
      DO 25 I=1,NN
   25 A3=A3+GNAGC(I)
      FNN=NN
      A3=A3/FNN
      DO 75 I=1,N
   75 AGC(I)=AGC(I)-A3
      CALL FITA2 (6,N,AGC,PSN,W,A1,B1,C1,PEA1,PEB1,PEC1,PEY1)
      DO 77 I=6,N
      DUM=A1+B1*AGC(I)+C1*(AGC(I)**2)
   77 ERR(I)=PSN(I)-DUM
      DO 76 I=1,N
   76 AGC(I)=AGC(I)+A3
C
C     CORRECTION FACTORS
```

```
C
      Y1C=A1
      YCC=Y1C+COR
C
C     FINAL PROBABLE ERRORS
C
      E3A=(CONST3+CONST4*(YDBAV **2)+CONST5+(2.0*CONST6))
      E3B=(1.0+1.0/(YRAV -1.0))**2
      E3D=(E3A*E3B)+(E2**2)+.00054562
      E3=SQRTF(E3D)
      E4=PEA2
      E5=SQRTF((E3**2)+(E4**2)*(CONST1**2))
      E6=PEA1
      IF (NN-3)99,98,98
   99 E7A=SQRTF(PEA1 **2+.04   )*CONST1
      GO TO 97
   98 PEA3=ZZ
      DO 43  I=1,NN
   43 PEA3=PEA3+((A3-GNAGC(I))**2)
      PEA3=.6745*(SQRTF(PEA3/(FNN-1.0)))
      E7A=SQRTF(PEA1 **2+(PEA3**2)*(B1 **2))*CONST1
   97 E7=SQRTF((E7A**2)+.0001407)
      E8=SQRTF((E7**2)+(E6**2)*(CONST1**2)+(E5**2))
C
C     NORMALIZED POWER LEVEL CORRECTED FOR ATMOSPHERE LOSS
C
      EFFR= 1.0/EFF
      AEF = CONST2*(ALOGF(EFFR))
      DO 15 I=1,NN
      TIME(I)=TIME(I)*24.0
      Y2C(I)=A1+B1*(GNAGC(I)-A3   )+C1*((GNAGC(I)-A3   )**2)
      ADB =(Y2C(I)+COR)+AEF
      ADBR= 10.0**(ADB/10.0)
      COSZ=((SINF(PHI*D)*SINF(DEC(I)*D))+(COSF(PHI*D)*COSF(DEC(I)*D)
     1   *COSF(HA(I)*D)))
      SECZ = 1.0/COSZ
      Z(I)= ATANF(SQRTF(SECZ**2 -1.0))*57.2957795
      ADBCR=ADBR*(XLO**SECZ)
      ADBC(I)=CONST2*(ALOGF(ADBCR))
   15 PEPP(I)=.01*SECZ
      IF (NN-3) 44,22,22
   44 NN=1
      A5=ADBC(1)
      B5=ZZ
      PEA5=PEPP(1)
      PEA5R=PEPP(1)*CONST1
      PEB5=ZZ
      PEY5=ZZ
      GO TO 46
   22 CALL FIT1 (NN,TIME,ADBC, PEPP,A5,B5,PEA5,PEB5,PEY5)
   46 EF=EFF*100.0
      PEA5R=PEA5*CONST1
      CAEF=A5
      CSISE=CAEF-(CONST2*ALOGF((PI*(SIZE**2)*.0929034)/4.0))
C
C     MORE PROBABLE ERRORS
C
      E9=(SQRTF((PEA5R**2)+.000193+.0085+(E8**2)))*CONST2
      E10=CONST2*(SQRTF(E7A**2+.02612   +(E6**2)*(CONST1**2)))
      EC1=PEYDBT
      EC2=E2*CONST2
```

```
      EC3=(SQRTF(E3A*E3B))*CONST2
      EC4=E3*CONST2
      EC5=E5*CONST2
      EC7=E7*CONST2
      EC8=E8*CONST2
C
C     PRINT INPUT DATA AND CORRECTIONS       *********    PAGE 1
C
      PRINT 11
      PRINT 19,TITLE
      PRINT 13,ITON,MONTH,NDAY,NYEAR,NYYN,NH
      PRINT 14,YA,TO,EF,GFSK,BWR,ALPHA,TS
      PRINT 26
      DO 27 I=1,5
   27 PRINT 28,I,AGC(I),PSN(I),ATT(I),PSY(I),ERR(I)
      DO 29 I=6,N
   29 PRINT 30,I,AGC(I),PSN(I),ERR(I)
      PRINT 31
      IF(NN-5)32,33,33
   32 DO 34 I=1,NN
   34 PRINT 35,I,GNAGC(I),TIME(I),Y2C(I),Z(I),YO(I),YE(I)
      J=NN+1
      DO 36 I=J,5
   36 PRINT 72,I,YO(I),YE(I)
      GO TO 85
   33 DO 38 I=1,5
   38 PRINT 35,I,GNAGC(I),TIME(I),Y2C(I),Z(I),YO(I),YE(I)
      DO 73 I=6,NN
   73 PRINT 35,I,GNAGC(I),TIME(I),Y2C(I),Z(I)
C
C     PRINT COMPUTED DATA                  ********       PAGE 2
C
   85 PRINT 60
      PRINT 61,A1,PEA1,A5,PEA5
      PRINT 62,B1,PEB1,B5,PEB5
      PRINT 63,C1,PEC1,PEY5
      PRINT 64,PEY1
      PRINT 65,COR
      PRINT 87
      PRINT 88,EC1
      PRINT 89,Y1C
      PRINT 90,EC2
      PRINT 91,E10
      PRINT 92,EC3
      PRINT 93,EC4 ,YCC
      PRINT 94,EC5,EC8
      PRINT 96,EC7
      PRINT 95,CAEF
      PRINT 91,E9
      PRINT 12,CSISE
C
C     SENSE SWITCH 2 ON FOR PUNCHED OUTPUT
C
      K=1
      IF (SENSE SWITCH 2)71,39
   71 PUNCH66,K,ITON,MONTH,NDAY,NYEAR,NYYN,NH,TS
      K=2
      PUNCH 70,K,NYYN,NH,Y1C,E10
      K=3
      PUNCH 70,K,NYYN,NH,YCC,EC8
      K=4
```

```
      PUNCH 70,K,NYYN,NH,CAEF,E9
      K=5
      PUNCH 70,K,NYYN,NH,CSISE
      GO TO 39
C
C     END OF PROGRAM INPUT FORMAT FOLLOWS
C
   10 FORMAT (I4,2I2,I4,F4.0,2F2.0,2X,F8.5,2F10.5,23X,I2)
   37 FORMAT (8F10.0)
   45 FORMAT (4F10.0,4F5.0,10X,F10.0)
   54 FORMAT(I4,2F2.0,2X,3F10.5)
   42 FORMAT (20A4)
C
C     OUTPUT FORMAT FOLLOWS                    *********
C
   52 FORMAT(11H TIME ERROR,E14.8,30H HOURS FROM TIME OF CALBRATION/
     151HCLEAR DATA FROM CARD READER, PUSH START, AND RELOAD/)
   11 FORMAT(1H1, 29X,41HC W    P O W E R    C A L I B R A T I O N//)
   19 FORMAT (10X,20A4/)
   14 FORMAT (5X,17HAIL-CAL REFERENCE,F6.2,3H DB,17H   AMB-LOAD TEMP.,
     1  F6.2,3H C ,13H    ANT. EFF.,F6.2,8H PERCENT// 5X,5HGFSK=,F8.2,
     23H DB,4X,4HBWR=,F10.3,4H CPS,4X,6HALPHA=,F5.3,3H DB,4X,3HTS=,
     3F6.2,8H DEGREES//)
   26 FORMAT (7X,4HDATA, 6X,3HAGC,4X,9HLEVEL SET,6X,4HDEV.,3X,
     4   21H AIL  ATT   CAL-POWER,5X,5HCORR./  7X,5HPOINT, 4X,5HVOLTS,
     56X,3HDBM,10X,2HDB,7X,3H DB,9X,3HDBM, 9X,2HDB/)
   28 FORMAT (6X,I4,2F11.2,11X,3F11.2)
   30 FORMAT (6X,I4,F11.2,2F11.2)
   13 FORMAT (6X,7HSTATION,I3,10X,4HDATE,I3,1H-,I2,1H-,I4,10X, 7HDAY NO.
     1,I4,5X,6HTIME  ,I4/)
   31 FORMAT (/// 7X,4HDATA,4X,6HSIGNAL,2X,10HNORMALIZED,3X,7HNOMINAL,
     12X,6HZENITH,7X,16HAIL-ATT  AIL-ATT/7X,5HPOINT,5X,3HAGC,6X,4HTIME,
     28X,3HDBM,4X,5HANGLE,10X,3HAMB,6X,3HSKY/)
   35 FORMAT (6X,I4,F11.2,F10.2,F11.2,F8.2,F14.2,F9.2)
   72 FORMAT (6X,I4,40X,F14.2,F9.2)
   60 FORMAT(1H1,21X,17HNOMINAL AGC CURVE,10X,21HRECEIVED SIGNAL SLOPE/)
   61 FORMAT (15X,2HA=,F10.5,5H  PE=,F10.5,5H   A=,F10.5,5H  PE=,F10.5)
   62 FORMAT (15X,2HB=,F10.5,5H  PE=,F10.5,5H   B=,F10.5,5H  PE=,F10.5)
   63 FORMAT (15X,2HC=,F10.5,5H  PE=,F10.5,15X,5H PEY=,F10.5)
   64 FORMAT (28X,4HPEY=,F10.5/)
   65 FORMAT (7X,18HCORRECTION FACTOR=,F10.3,3H DB/)
   87 FORMAT (11X,19HERROR CONTRIBUTIONS,14X,5H*****,14X,
     114HRECEIVED POWER/)
   88 FORMAT (13X,4HEC1=,F11.6)
   89 FORMAT (59X,8HNOMINAL=,F8.3,4H DBM)
   90 FORMAT (13X,4HEC2=,F11.6)
   91 FORMAT (64X,3HPE=,F8.3,3H DB)
   92 FORMAT (13X,4HEC3=,F11.6/)
   93 FORMAT (13X,4HEC4=,F11.6,28X,11HCALIBRATED=,F8.3,4H DBM/)
   94 FORMAT (13X,4HEC5=,F11.6,36X,3HPE=,F8.3,3H DB/)
   95 FORMAT (52X,15HINCIDENT POWER=,F8.3,4H DBM/)
   96 FORMAT (13X,4HEC7=,F11.6)
   12 FORMAT (/53X,14HPOWER DENSITY=,F8.3,13H DBM/SQ METER)
C
C     PUNCHED FORMAT              ********
C
   66 FORMAT (I2,6I6,2X,F15.4)
   70 FORMAT (I2,2I6,2X,2F15.5)
      END
```

```
      SUBROUTINE FIT1 (N,X,Y,W,A,B,PEA,PEB,PEY)
      DIMENSION X(15),Y(15),W(15)
      EN=N
      SW=0
      SWY=0
      SWXQ=0
      SWX=0
      SWXY=0
      SPY=0
      SPA=0
      SPB=0
      SPPY=0
      DO 100 I=1,N
      W(I)=(1.0/ W(I))**2
      SW=W(I)+SW
      SWX=W(I)*X(I)+SWX
      SWXQ=W(I)*(X(I)**2)+SWXQ
      SWY=W(I)*Y(I)+SWY
  100 SWXY=W(I)*X(I)*Y(I)+SWXY
      DELTA=SW*SWXQ-SWX**2
      A=(SWY*SWXQ-SWXY*SWX)/DELTA
      B=(SW*SWXY-SWX*SWY)/DELTA
      DO 200 I=1,N
      YC=A+B*X(I)
      E=YC-Y(I)
      SPY=W(I)*E*E +SPY
      SPPY=SPPY+ E*E
      SPA=W(I)*(SWXQ-X(I)*SWX)**2+SPA
  200 SPB=W(I)*(SWX-X(I)*SW)**2+SPB
      PEE=.6745*SQRTF(SPY/(EN-2.0))
      PEY=.6745*SQRTF(SPPY/(EN-2.0))
      CON=PEE/ABSF(DELTA)
      PEA=CON*SQRTF(SPA)
      PEB=CON*SQRTF(SPB)
      RETURN
      END
```

```
      SUBROUTINE FITA2 (NS,N,X,Y,W,A,B,C,PEA,PEB,PEC,PEY)
C     STELZRIED,2/18/66..WEIGHTED 2ND ORDER BEST FIT CURVE)
      DIMENSION X(100),Y(100),W(100)
      EN=N-NS+1
      SW=0
      SWX=0
      SWX2=0
      SWX3=0
      SWX4=0
      SWY=0
      SWXY=0
      SWX2Y=0
      DO 50 I=NS,N
      W(I)=(1./W(I))**2
      X2=X(I)*X(I)
      X3=X2*X(I)
      SW=W(I)+SW
      SWY=W(I)*Y(I)+SWY
      SWXY=W(I)*X(I)*Y(I)+SWXY
      SWX2Y=W(I)*X2*Y(I)+SWX2Y
      SWX=W(I)*X(I)+SWX
      SWX2=W(I)*X2+SWX2
      SWX3=W(I)*X3+SWX3
   50 SWX4=W(I)*X2*X2+SWX4
      A11=SWX2*SWX4-SWX3*SWX3
      A21=-(SWX*SWX4-SWX3*SWX2)
      A31=SWX*SWX3-SWX2*SWX2
      A22=SW*SWX4-SWX2*SWX2
      A32=-(SW*SWX3-SWX*SWX2)
      A33=SW*SWX2-SWX*SWX
      DELTA=SW*A11+SWX*A21+SWX2*A31
      A=(SWY*A11+SWXY*A21+SWX2Y*A31)/DELTA
      B=(SWY*A21+SWXY*A22+SWX2Y*A32)/DELTA
      C=(SWY*A31+SWXY*A32+SWX2Y*A33)/DELTA
      SPA=0
      SPB=0
      SPC=0
      SPY=0
      SPPY=0
      DO 75 I=NS,N
      X2=X(I)*X(I)
      YC=A+B*X(I)+C*X2
      E=YC-Y(I)
      SPY=W(I)*E*E+SPY
      SPPY=SPPY+E*E
      SPA=W(I)*(A11+X(I)*A21+X2*A31)**2+SPA
      SPB=W(I)*(A21+X(I)*A22+X2*A32)**2+SPB
   75 SPC=W(I)*(A31+X(I)*A32+X2*A33)**2+SPC
      PEE=.6745*SQRTF(SPY/(EN-3.0))
      PEY=.6745*SQRTF(SPPY/(EN-3.0))
      CON=PEE/ABSF(DELTA)
      PEA=CON*SQRTF(SPA)
      PEB=CON*SQRTF(SPB)
      PEC=CON*SQRTF(SPC)
      RETURN
      END
```

Appendix B
Discussion of the Computer Program

The data reduction is computed for each day's tracking at each station. The computer prints the following deviations and errors as well as the probable errors of the computed power levels:

(1) CORR DB. This column indicates the difference between each nominal test transmitter level and the corresponding calibrated value. The correction factor COR is the arithmetic mean of these values. These CORR differences form a powerful trouble-shooting tool.

(2) CORRECTION FACTOR. This is the power correction factor, COR.

(3) DEV DB. This column lists the deviations, in decibels, of each nominal test transmitter level from the statistical second-order nominal AGC curve.

(4) NOMINAL AGC CURVE. The three constants defining the computed nominal AGC curve are printed out under this heading. Their probable errors and the probable error of the individual data points are printed out as well. The probable error of the first constant A is used in the error analysis as the error caused by measurement scatter on the nominal curve.

(5) RECEIVED SIGNAL SLOPE. The two constants which define the computed straight line of received power versus normalized time, and their associated probable errors, are printed out under this heading. The probable error of the first constant A is used in the error analysis and the other probable errors (if $NN > 2$) are useful in trouble shooting.

(6) ERROR CONTRIBUTIONS. This lists some of the important contributions that make up the final errors. It is primarily a trouble-shooting and error-monitoring column. All probable errors in this column are in decibels.

(a) EC1. This is the measurement error associated with the Y-factors in the determination of system temperature.

(b) EC2. The probable error of the computed system temperature.

(c) EC3. The term

$$\left(\frac{PE_Y}{Y}\right)\left[1 + \frac{\alpha k T_s B}{P_{si}^* g(f_s)}\right]$$

in Eq. (11) is represented by this error contribution. It is the sensitivity of the error in the calibration of the test transmitter signal level to the Y-factors. Therefore, EC3 is the Y-factor error contribution to the calibration of the test transmitter (microwave thermal standards method).

(d) EC4. This is part of the probable error of the calibration of the test transmitter signal level by the microwave thermal standards method. It includes Y-factors, system temperature, bandwidth, filter gain, and diode correction factor; however, it does not include measurement scatter of data points. The probable error is described by Eq. (11).

(e) EC5. The complete probable error of the calibration of the test transmitter by the microwave thermal standards method.

(f) EC6. This is the same as E6, the error caused by the measurement scatter on the nominal AGC curve which has units of decibels. It is not listed because it is defined as PE_{A_1}, the probable error of the first constant of the computed nominal AGC curve. The term PE_{A_1} is listed under NOMINAL AGC CURVE.

(g) EC7. That portion of the probable error of the nominal spacecraft power, which is common to both nominal and calibrated methods.

(h) EC8. Probable error of the calibrated spacecraft power in decibels. This is printed in the computer output as PE corresponding to CALIBRATED power.

Appendix D shows a card-for-card type flow chart of the computer program and the subroutines.

Significant program statements for preliminary input are defined or discussed below:

Card No.	Definition or Discussion
5	XL0, assumed value of atmospheric loss at zenith at 2295 MHz, 1.011 579, ratio
6	D, converts radians to degrees
7	PI, π
8	CONST 1, $\ln 10/10 = 0.230\ 258\ 209\ 299$
9	CONST 2, $10/\ln 10 = 4.342\ 944\ 819\ 03$
10	CONST 3, $(a_1)^2 = 0.47717 \times 10^{-6}$, squared ratio
11	CONST 4, $(a_2)^2 = 0.6626 \times 10^{-6}$, $(\text{ratio/dB})^2$
12	CONST 5, $1/\tau B = 10^{-5}$, ratio
13	CONST 6, $(\Delta G/G_0)^2 = (\Delta P^*_{si}/P^*_{si})^2$ $= (0.005\ \text{dB})^2$ $= 2.5 \times 10^{-6}$, squared ratio
15	BK, Boltzmann's constant, $k = -198.60$ dB
19	Station input data: ITON, station number MONTH, NDAY, NYEAR, date DAYN, day of year H, FM, time; hours, min TO, ambient temperature, °C
20	Station constants: EFF, antenna efficiency, ratio TR, receiver equivalent noise temperature, °K GFS, overall normalized system gain at frequency f_s, ratio BWR, total integrated bandwidth of narrow-band filter, Hz ALPHA, diode correction factor, dB SA1, SA2, test transmitter step attenuator calibrations, dB SIZE, antenna physical diameter, ft PHI, antenna latitude, deg

Significant program statements for measured input are defined or discussed below:

Card No.	Definition or Discussion
21, 22	System temperature measurement data; Y-factors, dB
23	IF attenuator reference level for power calibration Y-factor, dB
25	AGC(I): first 5 AGC voltages, V PSN(I): first 5 nominal test transmitter levels, dBmW ATT(I): IF attenuator levels, dB
28	Nominal AGC curve: AGC(I): remainder of AGC voltages, V PSN(I): remainder of nominal test transmitter levels, dBmW
29	End of data card test
40	Received spacecraft power data: IDAY: day of year HRS, FMIN: time, hours, min GNAGC(I): ground receiver AGC voltage when the station has acquired the spacecraft, V
41	End of data card test

Significant program statements for time conversion and normalization are defined or discussed below:

Card No.	Definition or Discussion
32–38	Convert time to fractional days and normalize to calibration time, i.e., the time origin is placed at the time of calibration
43–46	Check that time in cards 40 through 45 has day number equal to day number ±1 day in card 19. This ensures that measurements of AGC voltage on the spacecraft (GNAGC) correspond to data read into the computer in statements 19 through 29. If time in statement 19 differs from time in statement 40 by more than 1 day, error message on cards 259 through 260 is typed, and the program returns to the start. A difference of 1 day is acceptable because the spacecraft may be tracked through midnight

Significant program statements for system temperature are defined or discussed below:

Card No.	Definition or Discussion
55, 56, 58, 62, and 64	Compute an average value of system temperature in °K by Eqs. (34) and (36)
59–61	Compute the probable error of the average system temperature Y-factor in decibels from Eq. (37), i.e., $PE_{\overline{Y}_{a0}}$ (PEYDBT in the program)

Card No.	Definition or Discussion
63	Converts $PE_{\bar{Y}_{a0}}$ to a normalized ratio by Eq. (38). The result is symbolized E1 in the program
65	Converts the temperature of the ambient load from °C to °K
66–68	Compute the probable error of the system temperature measurement by Eqs. (35) and (39). The result is symbolized E2 in the program

Significant program statements for calibration of the test transmitter signal level are defined or discussed below:

Card No.	Definition or Discussion
72	Converts bandwidth in hertz to decibels
73	Converts system temperature in degrees K to decibels
74	Computes the term GFSK and converts it to decibels, where $$\mathrm{GFSK} = k/g(f_s)$$ and $$k = \text{Boltzmann's constant, } J/°\mathrm{K}$$ $$g(f_s) = \text{is defined by Eq. (4)}$$
75	Computes the term TGB in decibels, where TGB is given by $T_s B/g(f_s)$
78	Computes the calibration Y-factors YDB(I), by YDB(I) = ATT(I) − YA
79	Converts the Y-factors YDB(I) to ratios, YR
80, 82	Solve Eq. (7) for five calibrated test transmitter power levels PSY(I). These points are needed to determine the calibrated AGC curve
83	Computes the differences between the nominal and calibrated test transmitter power levels, PSY(I) − PSN(I). These five differences are printed under CORR DB for each day's data

Significant program statements for step attenuator rection are defined or discussed below:

Card No.	Definition or Discussion
86–95	Correct the nominal test transmitter power levels by the factors SA1 and SA2

Significant program statements for the power correction factor COR and its probable error are defined or discussed below:

Card No.	Definition or Discussion
81, 84, and 85	Compute the average Y-factor, and convert it to a ratio
96–102	Compute COR, the average difference between PSY(I) and PSN(I)
103–106	Compute the normalized probable error ratio PE_{COR}/COR. This is given by: $$\left(\frac{PE_{COR}}{COR}\right)^2 = (PE_{A_2})^2 \cdot (\mathrm{CONST\ 1})^2 \qquad (58)$$ where PE_{A_2} is given by: $$0.6745 \left\{ \frac{\sum_i [\mathrm{COR} - (\mathrm{PSY(I)} - \mathrm{PSN(I)})]^2}{N - 1 = 4} \right\}^{1/2} \mathrm{dB} \qquad (59)$$

Significant program statements for the nominal AGC curve are defined or discussed below:

Card No.	Definition or Discussion
110	Changes NN to FNN to avoid a mixed mode in 111
107–109, and 111	Determine the number NN of GNAGC data points and compute their average. This determines the reference point on the AGC axis to which the origin is to be moved. This reference point is the first GNAGC data point for NN≦2 and the average GNAGC value for NN > 2
112, 113	Transform the Y-axis to the reference point

Card No.	Definition or Discussion
114	Calls the subroutine FITA2 which fits the best second-order curve to the nominal AGC curve data from $i = 6$ to a data point above threshold ($i = N$). The constants A_1, B_1, C_1 of the curve $Y = A_1 + B_1x + C_1x^2$ are determined where Y = power in dBmW, and x = AGC voltage. The subroutine also determines PE_{A_1}, PE_{B_1}, PE_{C_1}, and PE_{Y_1} where PE_{Y_1} is the probable error of the individual data points
115–117	Determine the deviation of each nominal AGC data point from $i = 6$ to $i = N$ from the corresponding point on the computed curve $Y = A_1 + B_1x + C_1x^2$
118, 119	Reset the AGC voltage data to the original origin

Significant program statements for the nominal and calibrated spacecraft power levels are defined or discussed below:

Card No.	Definition or Discussion
123	Determines the nominal value of received spacecraft power level, Y1C. This is given by the constant A_1 which was found in card 114 through the subroutine
124	Computes the calibrated spacecraft power level YCC = Y1C + COR

Significant program statements for the probable error of the calibration of the test transmitter level are defined or discussed below:

Card No.	Definition or Discussion
128	Computes the term E3A where $\mathrm{E3A} = (a_1)^2 + (a_2 Y_{\mathrm{dB}})^2 + \frac{1}{\tau B} + \left(\frac{\Delta G}{G_0}\right)^2 + \frac{\Delta P^*_{si}}{P^*_{si}}$ and is part of Eq. (11)
129	Computes the term E3B where $\mathrm{E3B} = \left(1 + \frac{1}{\mathrm{YRAV} - 1}\right)^2$ The term $\left(1 + \frac{\alpha k T_s B}{P^*_{si}\, g(f_s)}\right)$ in Eq. (11) may be written 1 + 1/(YRAV − 1), where YRAV is the average power Y-factor converted to a ratio
130	Computes the term E3D where $\mathrm{E3D} = (\mathrm{E3A})(\mathrm{E3B}) + (\mathrm{E2})^2 + 0.000545\ 620$ PE$_\alpha$ was estimated as 0.1 dB. This could probably be reduced in future systems. $PE_{g(f_s)}/g(f_s)$ was estimated as 0.003 (ratio) and PE_B/B was 0.0026 (ratio) on the average. Hence, $\left(\frac{PE_\alpha}{\alpha}\right)^2 + \left[\frac{PE_{g(f_s)}}{g(f_s)}\right]^2 + \left(\frac{PE_B}{B}\right)^2 = 0.000545\ 620$
131	Computes the term E3 where $\mathrm{E3} = (\mathrm{E3D})^{1/2}$
132	Defines E4 as PE_{A_2}
133	Computes the probable error of the calibration of the test transmitter power level (microwave thermal standards method). This is defined as E5, where $(\mathrm{E5})^2 = (\mathrm{E3})^2 + (\mathrm{E4})^2 (\mathrm{CONST\ 1})^2$

Significant program statements for common errors are defined or discussed below:

Card No.	Definition or Discussion
134	Defines E6 as PE_{A_1}
135	Condition. Directs the program according to the number of GNAGC data points
136	If NN $\leq$ 2, this statement is used. It computes the term E7A where $(\mathrm{E7})^2 = (\mathrm{CONST\ 1})^2 [(PE_{A_1})^2 + (0.2)^2]$ Since NN is not sufficiently great to perform a first-order analysis, the term $(PE_x)(B_1)$ in Eq. (47) must be estimated. This term has been estimated as 0.2 dB. The program then jumps to card 143
140, 141	If NN > 2, then these statements are used. These statements compute PE_{A_3} by Eq. (49)

Card No.	Definition or Discussion
142	Computes the term E7A where $(\text{E7A})^2 = [(PE_{A_1})^2 + (PE_{A_3})^2 (B_1)^2] (\text{CONST 1})^2$ from Eq. (47). The units PE_{A_1} are in decibels; those of PE_{A_3} are in volts; those of B_1, decibels/volts; and CONST 1 converts E7A to a ratio
143	Computes the term E7 where $$(\text{E7})^2 = (\text{E7A})^2 + \sum_{i=3}^{7} (a_i)^2$$ and $(a_i)^2 = 0.000\ 1407$ (ratio)^2. The term E7 is the summation of all errors common to both methods

Significant program statements for the probable error of the calibrated spacecraft power level are defined or discussed below:

Card No.	Definition or Discussion
144	Computes the term E8, the probable error of the calibrated spacecraft power level

Significant program statements for spacecraft power level normalized for 100% antenna efficiency are defined or discussed below:

Card No.	Definition or Discussion
148, 149	Convert antenna efficiency to decibels. This is given by the term AEF. The reciprocal of antenna efficiency is used to keep AEF positive.
152	Computes NN values of nominal spacecraft power by solving the equation defining the nominal curve for each of the NN values of GNAGC voltage. $$\text{Y2C(I)} = A_1 + B_1 [\text{GNAGC(I)} - A_3] + C_1 [\text{GNAGC(I)} - A_3]^2$$ where Y2C is the nominal received power and A_3 is given by Eq. (48)
153	Computes NN values of ADB where $$\text{ADB} = \text{Y2C(I)} + \text{COR} + \text{AEF}$$ ADB represents NN values of received spacecraft power, calibrated and normalized for 100% antenna efficiency

Card No.	Definition or Discussion
154	Converts the NN values of ADB found in card 153 from dBmW to ratios. These ratios are designated ADBR

Significant program statements for spacecraft power level corrected for atmospheric loss are defined or discussed below:

Card No.	Definition or Discussion
155, 156	Compute cos z from Eq. (28)
157	Computes sec z from cos z
158	Computes z(I) in degrees which are held and printed in the output
159	Computes NN values of ADBCR by Eq. (9) $$\text{ADBCR} = (\text{ADBR})(L_0)^{\sec z}$$ where ADBCR are the values of ADBR corrected for atmospheric loss
160	Converts the NN values of ADBCR to decibels

Significant program statements for incident power are defined or discussed below:

Card No.	Definition or Discussion
161	Defines the weighting factors for the straight-line analysis. These are given by Eq. (56) as: $$w = \left[\left(\frac{PE_{L_0}}{L_0}\right) \cdot \sec z\right]^{-2}$$ The term L_0 has been chosen as 0.05 dB and PE_{L_0}/L_0 was estimated as 0.01. The subroutine FITA2 uses the square of the reciprocal of the input weighting factors and, therefore, card 161 of the program defines the weighting factors as $w^{-1/2}$
162	Determines whether there are sufficient data points to perform a first-order statistical analysis, and directs the program to cards 163 through 170 if there are not, and to card 171 if there are
163	Defines NN as 1, i.e., the first data point is chosen
164	The term A_5 is defined as ADBC(1), i.e., the first value of ADBC

Card No.	Definition or Discussion
166	Defines PE_{A_5} as PEPP(1), i.e., the first weighting factor
167	Converts PEPP(1) to a ratio
171	Calls the subroutine FIT1 which fits a straight line to the NN data points of ADBC versus time in the original coordinate system, by a least-squares method using the defined weighting factors. The subroutine computes the values of the constants A_5 and B_5 as well as the probable errors PE_{A_5}, PE_{B_5}, PE_{Y_5}
172	Antenna efficiency as a percentage is defined as EF. This is held and printed in the output
173	Converts PE_{A_5} to a ratio
174	Defines incident power as A_5, where A_5 = CAEF
175	Computes incident power density as received signal strength per square meter of antenna aperture. This is designated CSISE

Significant program statements for probable error of incident power are defined or discussed below:

Card No.	Definition or Discussion
179	Computes the term E9 by Eq. (57)

Significant program statements for probable error of the nominal spacecraft power are defined or discussed below:

Card No.	Definition or Discussion
180	The probable error of the nominal spacecraft power is defined as E10 where $(\mathrm{E10})^2 = (\mathrm{CONST\ 2})^2 [(\mathrm{E7A})^2 + 0.02612 + (\mathrm{E6})^2 (\mathrm{CONST\ 1})^2]$ The units of E10 are decibels. The term E7A is given by card 136. The term 0.02612 is a squared ratio and is given by $0.02612 = (PE_{TTC})^2 + \sum_{i=3}^{7} (a_i)^2$ where PE_{TTC} = probable error of the test transmitter signal level calibration by the nominal method, estimated as 0.7 dB and $\Sigma (a_i)^2$ is defined in card 143

Appendix C

The Diode Correction Factor

The diode correction factor α was determined by comparisons of Y-factors, Y_d and Y_p, measured with the diode and a true rms detector, respectively, at the same signal-to-noise ratio. A theoretical analysis was also performed to gain insight into the phenomenon and to provide a check on the calibrations. The theoretical analysis is considered in this appendix.

I. Definitions

A representation of the 1N198 diode detector circuit used in the power Y-factor measurements is shown in Fig. C-1. Because of the difference in form factor, equal CW and noise powers do not result in equal rectified output voltages.

A block diagram of the diode detector system used for the power Y-factor measurements is shown in Fig. C-2. Assuming unequal output indicator responses E_{sn} and E_n caused by detector inputs of signal combined with noise $(P_{sn})_i$ and noise power alone $(P_n)_i$, proportional to β

$$\frac{E_{sn}}{E_n} = \beta' \frac{(P_{sn})_i}{(P_n)_i} \tag{60}$$

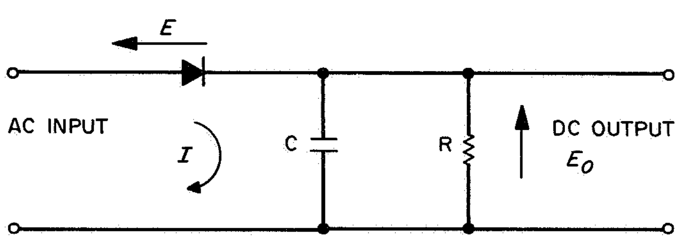

Fig. C-1. Representation of diode detector circuit used in Y-factor measurements

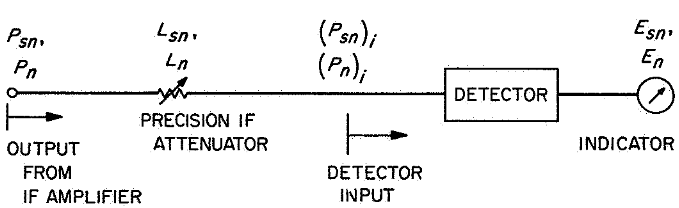

Fig. C-2. Detector system used in Y-factor measurements

When taking Y-factor measurements, the precision IF attenuator is adjusted for attenuations L_{sn} and L_n, to give equal output indicator deflections resulting in a ratio

$$Y_d = L_{sn}/L_n \tag{61}$$

so that

$$E_{sn}/E_n = 1 \tag{62}$$

The correction factor under these conditions is then

$$\beta = \frac{(P_n)_i}{(P_{sn})_i} \tag{63}$$

The signal, plus noise-to-noise ratio before and after the attenuator, are related by

$$\frac{1}{Y_d} \cdot \frac{P_{sn}}{P_n} = \frac{(P_{sn})_i}{(P_n)_i} \tag{64}$$

so that

$$Y_d = \beta \frac{P_{sn}}{P_n} \tag{65}$$

or, if P_{sn} is written $P_s + P_n$,

$$Y_d = \beta \left(1 + \frac{P_s}{P_n} \right) \tag{66}$$

The relative diode sensitivity to signal and noise can also be expressed as

$$Y_d = 1 + \frac{P_s}{\alpha P_n} \tag{67}$$

β is related to α by

$$\alpha = \frac{P_s/P_n}{\beta (P_s/P_n + 1) - 1} \tag{68}$$

or, if $P_s/P_n >> 1$

$$\alpha \approx 1/\beta \approx \frac{(P_s)_i}{(P_n)_i} \tag{69}$$

II. Effect of Low Signal-to-Noise Ratio and Bias

The detector can be analyzed to a first approximation as a ν^{th} law device to indicate the effect of combining signal and noise, which is of importance if P_s/P_n is not large. It is assumed that there is no reverse current, no bias, and no ν^{th} law response as shown in Fig. C-3.

The no-bias requirement is closely satisfied if the peak input signal level is much greater than the dc output voltage. The dc output with signal and noise is (Ref. 10):

$$E_{on} = \left[\frac{a\Gamma(\nu+1)}{\Gamma(\nu/2+1)\,2^{\nu/2+1}}\right](P'_n)^{\nu/2}\,{}_1F_1 \times\left[-\frac{\nu}{2}:1:\frac{(P_s)_i}{(P'_n)_i}\right] \tag{70}$$

and, with noise alone,

$$E_n = \left[\frac{a\Gamma(\nu+1)}{\Gamma(\nu/2+1)\,2^{\nu/2+1}}\right](P_n)^{\nu/2}\,{}_1F_1\left[-\frac{\nu}{2}:1:0\right] \tag{71}$$

where

a = proportionality factor

ν = detector law

Γ = gamma function

${}_1F_1$ = confluent hypergeometric function

$(P_s)_i/(P'_n)_i$ = CW signal-to-noise power ratio at the detector input

and

$$(P_{sn})_i = (P'_n)_i + (P_s)_i$$

Dividing Eq. (70) by Eq. (71), ${}_1F_1(-\nu/2:1:0) = 1$ since

$$\frac{E_{sn}}{E_n} = \left[\frac{(P'_n)_i}{(P_n)_i}\right]^{\nu/2}{}_1F_1\left[-\frac{\nu}{2}:1:-\frac{(P_s)_i}{(P_n)_i}\right] \tag{72}$$

Using Eqs. (63) through (65) and, since

$$\frac{(P'_n)_i}{(P_n)_i} = \frac{1}{Y_d} \tag{73}$$

then,

$$\frac{(P_s)_i}{(P'_n)_i} = \frac{P_s}{P_n} \tag{74}$$

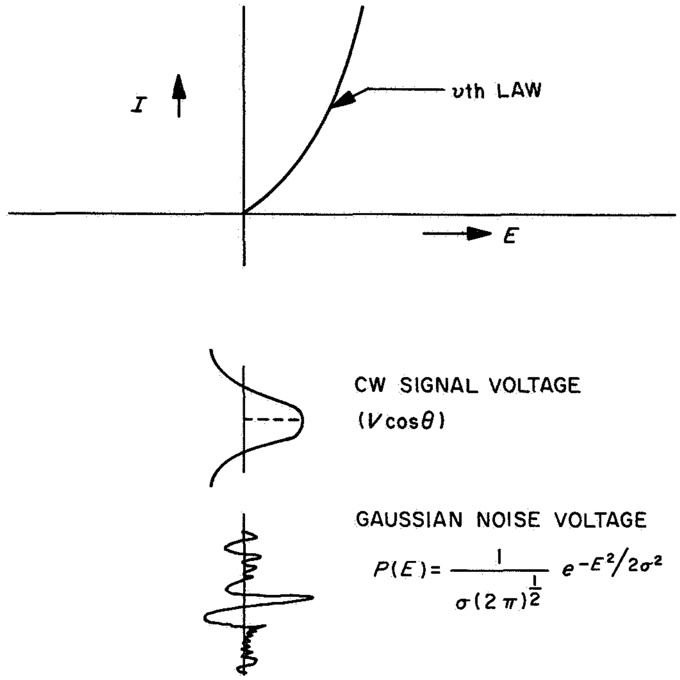

Fig. C-3. Representation of ideal ν^{th} law diode characteristic

and

$$\frac{(P'_n)_i}{(P_n)_i} = \frac{1}{\beta\left(\dfrac{P_s}{P_n}+1\right)} \tag{75}$$

Using Eqs. (68), (74), and (75) with Eq. (72), and setting $E_{sn}/E_n = 1$,

$$1 = \left(\frac{P_s}{\alpha P_n}+1\right)^{-\nu/2}{}_1F_1\left(-\frac{\nu}{2}:1:-\frac{P_s}{P_n}\right) \tag{76}$$

The relationship between α and $(P_s)/(P_n)$ is shown by this equation. The confluent hypergeometric function can be expanded in a power series for large signal-to-noise ratios (Ref. 11). Equation (76) has been programmed for a computer, and α was determined and plotted for a range of values for ν and for P_s/P_n ratios, as shown in Fig. C-4. This shows that ideal ν^{th} law detectors with nonlinearities reasonably close to square law have relatively small corrections for the Y-factor.

III. Direct Method

The circuit shown in Fig. C-1 can be analyzed by a direct method to determine the sensitivity to a CW signal alone, as compared to a noise signal. The dc output volt-

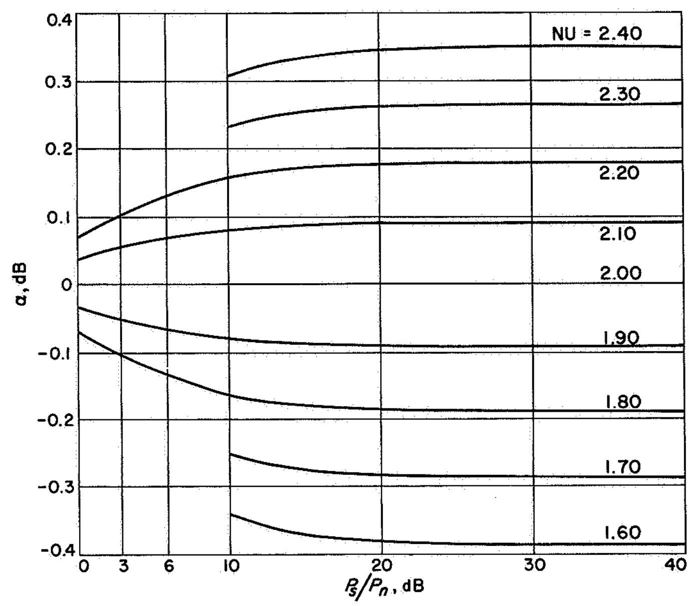

Fig. C-4. Plot of α (dB) vs P_s/P_n from Eq. (76)

age, using the same assumptions and with an input signal $V \cos \theta$, is given by

$$(E_0)_s = R \langle I \rangle_s \tag{77}$$

If the relation that $I = aE^\nu$ for $E > 0$ is used,

$$\langle I \rangle_s = \langle aE^\nu \rangle_s = \frac{a}{\pi} \int_0^{\pi/2} (V \cos \theta)^\nu \, d\theta \tag{78}$$

By integrating (Ref. 12) and substituting into Eq. (77)

$$(E_0)_s = \frac{aRV^\nu \Gamma\left(\frac{\nu}{2} + \frac{1}{2}\right)}{2(\pi)^{1/2} \Gamma\left(\frac{\nu}{2} + 1\right)} \tag{79}$$

Replacing the peak voltage V with an effective rms voltage v where

$$\frac{V^2}{2} = v^2$$

then,

$$(E_0)_s = \frac{aR(2v^2)^{\nu/2} \Gamma\left(\frac{\nu}{2} + \frac{1}{2}\right)}{2(\pi)^{1/2} \Gamma\left(\frac{\nu}{2} + 1\right)} \tag{80}$$

The average dc output voltage caused by a noise input voltage is

$$(E_0)_n = R \langle I \rangle_n \tag{81}$$

where (Ref. 13)

$$\langle I \rangle_n = \langle aE^\nu \rangle_n = a \int_{-\infty}^{\infty} E^\nu P(E) \, dE \tag{82}$$

Assuming a gaussian noise input with an rms noise voltage σ

$$P(E) = \left[\frac{1}{\sigma(2\pi)^{1/2}}\right] e^{-E^2/2\sigma^2}$$

so that

$$\langle I \rangle_n = \frac{a}{\sigma(2\pi)^{1/2}} \int_0^{\infty} E^\nu e^{-E^2/2\sigma^2} \, dE \tag{83}$$

Integrating and substituting into Eq. (81)

$$(E_0)_n = \left[\frac{aR(2\sigma^2)^{\nu/2}}{2(\pi)^{1/2}}\right] \Gamma\left(\frac{\nu}{2} + \frac{1}{2}\right) \tag{84}$$

Dividing Eq. (79) by Eq. (84) and setting $(E_0)_s/(E_0)_n = 1$ yields

$$1 = \left(\frac{v^2}{\sigma^2}\right)^{\nu/2} \left[\frac{1}{\Gamma\left(\frac{\nu}{2} + \frac{1}{2}\right)}\right] \tag{85}$$

But, since

$$\frac{(P_s)_i}{(P_n)_i} = \left[\Gamma\left(\frac{\nu}{2} + 1\right)\right]^{2/\nu} \tag{86}$$

and, with Eqs. (63) and (69) for the ideal ν^{th} law detector assuming $P_s/P_n >> 1$,

$$\alpha = \left[\Gamma\left(\frac{\nu}{2} + 1\right)\right]^{2/\nu} \tag{87}$$

Equation (76) asymptotically approaches Eq. (87) as $P_s/P_n \rightarrow \infty$. Figure C-4 indicates that good accuracy for α can be obtained for signal-to-noise ratios above 10 dB, which is the range of the measurements used for the spacecraft CW power calibrations.

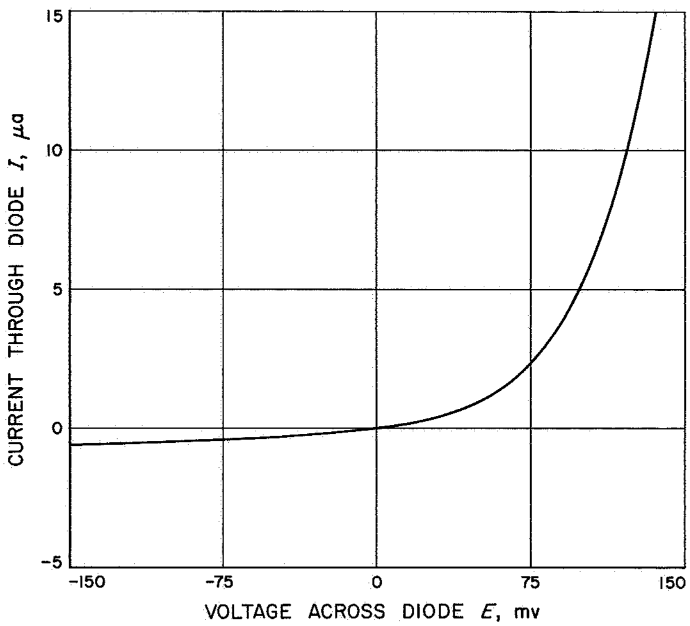

Fig. C-5. Echo station detector diode static E I characteristic, run 15, 24.20°C

The effect of bias can be estimated assuming an ideal square law diode response and $E_0 << \sigma$ and $\nu = 2$, as shown in Fig. C-5. This bias is caused by the long time constant compared to the period of R and C shown in Fig. C-1. With an input signal $V \cos \theta$, the dc output voltage is given by (Eq. 77)

$$(E_0)_s = R\langle I\rangle_s$$

For this example

$$I = aE^2 \qquad \text{for } E > 0$$

Thus,

$$\langle I\rangle_s = \langle aE^2\rangle = \frac{a}{\pi}\int_0^{\theta_1} (V\cos\theta - E_0)^2\, d\theta$$

$$= \frac{aV^2}{\pi}\int_0^{\theta_1}\left(\cos\theta - \frac{E_0}{V}\right)^2 d\theta \tag{88}$$

where

$$\theta_1 = \cos^{-1}\frac{E_0}{V}$$

$$\approx \frac{\pi}{2} - \frac{E_0}{V} \qquad \text{for } E_0/V << 1$$

Expanding Eq. (88), integrating, and retaining the first-order correction term,

$$\langle I\rangle_s \approx \frac{aV^2}{\pi}\left(\frac{\pi}{4} - \frac{2E_0}{V}\right) \tag{89}$$

so that replacing V with $v(2)^{1/2}$ and substituting into Eq. (77) yields

$$(E_0)_s \approx \frac{aRv^2}{2}\left(1 - \frac{8E_0}{\pi v(2)^{1/2}}\right) \tag{90}$$

The average dc output voltage caused by a noise input voltage is

$$(E_0)_n = R\langle I\rangle_n \tag{91}$$

where

$$\langle I\rangle_n = \langle aE^2\rangle_n = a\int_0^\infty E^2 P(E)\, dE \tag{92}$$

Assuming a gaussian noise input with an rms noise voltage σ and a bias $(-E_0)$ (Ref. 13),

$$P(E) = \left(\frac{1}{\sigma(2\pi)^{1/2}}\right)e^{-(E+E_0)^2/2\sigma^2} \tag{93}$$

Then,

$$\langle I\rangle_n = \frac{a}{\sigma(2\pi)^{1/2}}\int_0^\infty E^2 e^{-(E+E_0)^2/2\sigma^2}\, dE \tag{94}$$

Substituting $x = E + E_0$,

$$\langle I\rangle_n = \frac{a}{\sigma(2\pi)^{1/2}}\int_{E_0}^\infty (x - E_0)^2 e^{-x^2/2\sigma^2}\, dx \tag{95}$$

which may be written as

$$\langle I\rangle_n = \frac{a}{\sigma(2\pi)^{1/2}}\left[\int_0^\infty (x - E_0)^2 e^{-x^2/2\sigma^2}\, dx - \int_0^{E_0} (x - E_0)^2 e^{-x^2/2\sigma^2}\, dx\right] \tag{96}$$

Expanding the second integrand, integrating both integrals, and retaining only first-order terms,

$$\langle I\rangle_n \approx \frac{a}{\sigma(2\pi)^{1/2}}\left[\frac{\sigma^3}{2}(2\pi)^{1/2} - 2\sigma E_0\right] \tag{97}$$

Substituting into Eq. (91)

$$(E_0)_n \approx \frac{aR\sigma^2}{2}\left[1 - \frac{4E_0}{\sigma(2\pi)^{1/2}}\right] \tag{98}$$

Dividing Eq. (90) by Eq. (98) and setting equal to 1

$$1 \approx \left(\frac{v^2}{\sigma^2}\right)\frac{1 - \dfrac{8E_0}{v(2\pi)^{1/2}}}{1 - \dfrac{4E_0}{\sigma(2\pi)^{1/2}}} \tag{99}$$

substituting α for v^2/σ^2

$$\alpha \approx 1 + \left(\frac{E_0}{v}\right)\left(\frac{4}{(2\pi)^{1/2}}\right)\left(\frac{2}{(\pi)^{1/2}} - 1\right) + \cdots \tag{100}$$

If $E_0/\sigma \approx E_0/v \approx 1\,|\,10$ (the approximate operating range of the diode detectors when taking Y-factors), then $\alpha \approx 0.1$ dB. This indicates the relative importance of bias effects on the calibrations.

IV. Analysis From the Diode Static EI Curve

This analysis, which takes bias into account, predicts the sensitivity to CW and noise signals from the diode dc current and voltage characteristics.

If it is assumed that the diode current I can be expressed in terms of the voltage across the diode E, by the power series

$$I = \sum_{i=0}^{N} A_i E^i \tag{101}$$

The circuit ac input voltage e is related to output dc voltage E_0, by

$$e = E + E_0 \tag{102}$$

because of the biasing effect of the output $R - C$ local combination with an $R - C$ time constant which is long compared to the input frequency. The current can also be expressed as a power series in terms of the circuit input voltage

$$I = \sum_{i=0}^{N} C_i e^i \tag{103}$$

Substituting Eq. (102) into Eq. (101), expanding Eqs. (101) and (103), and equating coefficients of like powers of e yields

$$\begin{aligned}
C_0 &= A_0 - A_1E_0 + A_2E_0^2 - A_3E_0^3 + A_4E_0^4 - A_5E_0^5 + A_6E_0^6 \\
&\quad - A_7E_0^7 + A_8E_0^8 + \cdots \\
C_2 &= A_2 - 3A_3E_0 + 6A_4E_0^2 - 10A_5E_0^3 + 15A_6E_0^4 \\
&\quad - 21A_7E_0^5 + 28A_8E_0^6 + \cdots \\
C_4 &= A_4 - 5A_5E_0 + 15A_6E_0^2 - 35A_7E_0^3 + 70A_8E_0^4 + \cdots \\
C_6 &= A_6 - 7A_7E_0 + 28A_8E_0^2 + \cdots \\
C_8 &= A_8 + \cdots
\end{aligned} \tag{104}$$

With a CW input signal $V\cos\theta$, the average current in the circuit is

$$\left.\begin{aligned}
\langle I\rangle_s &= \frac{1}{2\pi}\int_0^{2\pi} I\,d\theta = \frac{1}{\pi}\int_0^{\pi}\sum_{i=0}^{N} C_i(V\cos\theta)^i\,d\theta \\
&= C_0 + \frac{1}{2}C_2V^2 + \frac{3}{8}C_4V^4 + \frac{E}{R}C_6V^6 \\
&\quad + \frac{35}{128}C_8V^8 + \cdots
\end{aligned}\right\} \tag{105}$$

The dc output voltage is related to the load resistor R, by

$$(E_0)_s = R\langle I\rangle_s \tag{106}$$

Substituting Eq. (105) into Eq. (106), and replacing the peak voltage V by $v(2)^{1/2}$, where v is the effective value of the sinusoid

$$\begin{aligned}
(E_0)_s = R\bigg(C_0 + C_2v^2 + \frac{3}{2}C_4v^4 + \frac{5}{2}C_6v^6 \\
+ \frac{35}{2}C_8v^8 + \cdots\bigg)
\end{aligned} \tag{107}$$

With a noise input, the average current in the circuit is (Ref. 13)

$$\langle I\rangle_n = \int_{-\infty}^{D} I(e)\,P(e)\,de \tag{108}$$

where

$$P(e) = \left(\frac{1}{\sigma(2\pi)^{1/2}}\right) \xi^{-e^2/2\sigma}$$

$$I(e) = \sum_{i=0}^{N} C_i e^i$$

Substituting for $P(e)$ and $I(e)$, and integrating

$$\langle I \rangle_n = C_0 + C_2\sigma^2 + 3C_4\sigma^4 + 15C_6\sigma^6 + 105C_8\sigma^8 + \cdots \tag{109}$$

The dc output is given by (Eq. 81)

$$(E_0)_n = R\langle I \rangle_n$$

or

$$(E_0)_n = R(C_0 + C_2\sigma^2 + 3C_4\sigma^4 + 15C_6\sigma^6 + 105C_8\sigma^8 + \cdots) \tag{110}$$

It should be noted that the detector output voltages, because of a CW signal and noise (as given by Eqs. 107 and 110), differ with respect to each other only in the voltage coefficients higher than second order.

The sensitivity of the diode correction factor α, to a CW signal versus noise at a specified dc output level E_0, is obtained by solving for v and σ from Eqs. (107) and (110), and substituting into (assuming high signal-to-noise ratios)

$$\alpha = \left(\frac{v}{\sigma}\right)^2 \tag{111}$$

This was done for the detector diodes from the Echo and Pioneer stations. As an example, the static voltage–current characteristic (Run 15 at 24.20°C) for the Echo station is shown with a best-fit curve in Fig. C-5. The polynomial eighth-order curve fit was obtained by a least-squares method using a computer. The A coefficients (defined by Eq. 101) are:

A coefficients	Values
0	$0.56971715 \times 10^{-2}$
1	$0.94633774 \times 10^{-2}$
2	$0.10920516 \times 10^{-3}$
3	$0.11652644 \times 10^{-5}$
4	$0.10032540 \times 10^{-7}$
5	$0.64969665 \times 10^{-10}$
6	$0.26946926 \times 10^{-12}$
7	$0.61865139 \times 10^{-15}$
8	$0.59703929 \times 10^{-18}$

The standard deviation of the data points was 0.02017. Polynomial curve fits of various orders were tried to determine the optimum fit, as defined by the minimum standard deviation. The eighth-order fit was suitable, consistent with minimizing the number of constants to simplify the solution. The terms I and E for the curve fit are in microamperes and millivolts. The C coefficients were computed by using Eq. (104) for each output voltage E_0, and α was computed from Eq. (111) with Eqs. (107) and (110). These computations were made with a computer. For this case, the following tabulation applies:

E_0, mV	v, mV	σ, mV	α, dB
2	30.2948	28.7869	0.443
4	42.0678	38.8203	0.698

This indicates a sensitivity of α to the output level of approximately 0.013 dB/0.1 mV for this diode at the output level of 4 mV.

Appendix D

Flow Chart of the Computer Program

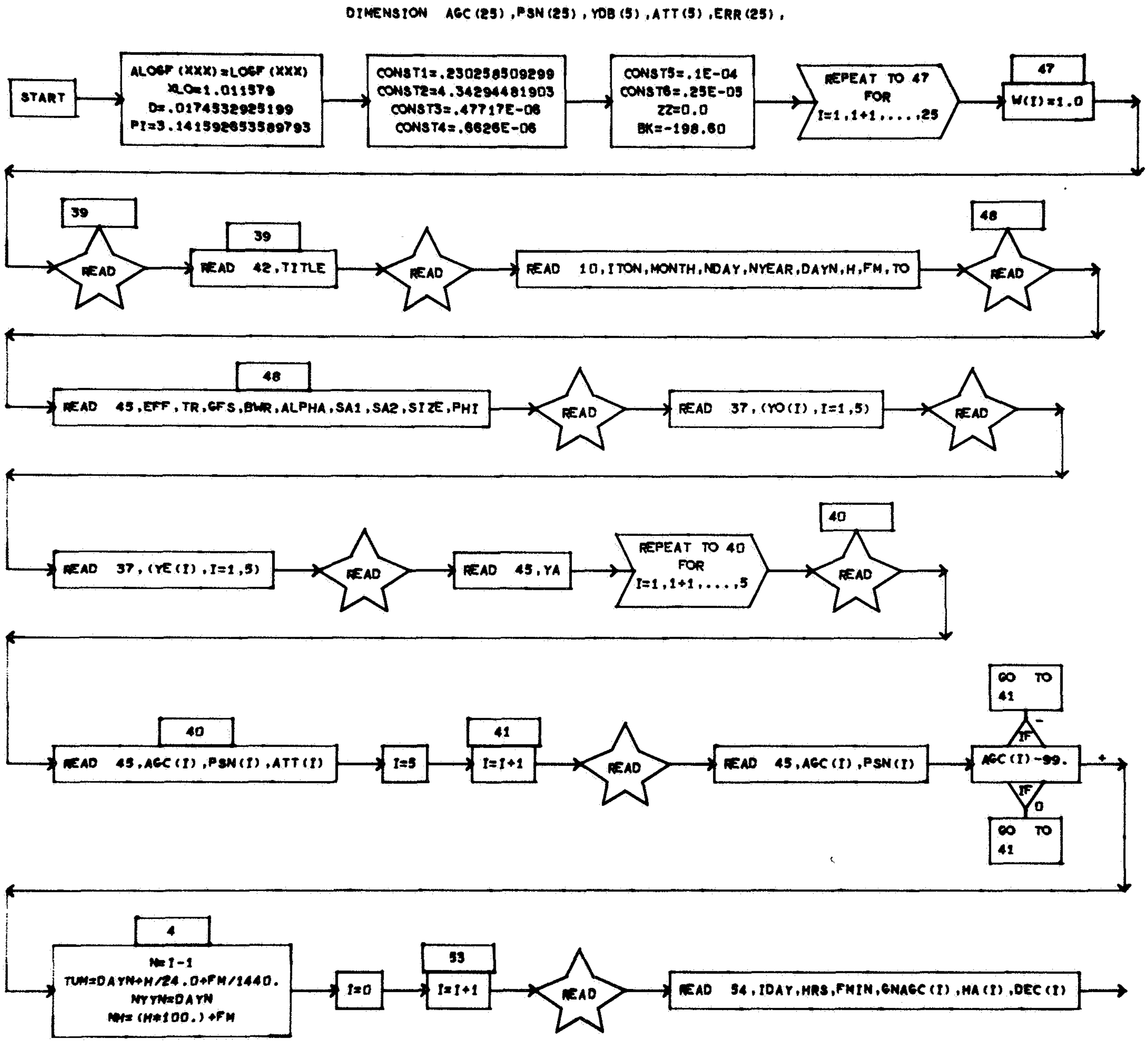
DIMENSION AGC(25),PSN(25),YOB(5),ATT(5),ERR(25),
START
ALOGF(XXX)=LOGF(XXX)
XLO=1.011579
D=.0174532925199
PI=3.14159265358979З
CONST1=.230258509299
CONST2=4.34294481903
CONST3=.47717E-06
CONST4=.6626E-06
CONST5=.1E-04
CONST6=.25E-05
ZZ=0.0
BK=-198.60
REPEAT TO 47 FOR I=1,1+1,....,25
47
W(I)=1.0
39
READ
39
READ 42,TITLE
READ
READ 10,ITON,MONTH,NDAY,NYEAR,DAYN,H,FM,TO
48
READ
48
READ 45,EFF,TR,GFS,BWR,ALPHA,SA1,SA2,SIZE,PHI
READ
READ 37,(YO(I),I=1,5)
READ
READ 37,(YE(I),I=1,5)
READ
READ 45,YA
REPEAT TO 40 FOR I=1,1+1,....,5
40
READ
40
READ 45,AGC(I),PSN(I),ATT(I)
I=5
41
I=I+1
READ
READ 45,AGC(I),PSN(I)
GO TO 41
IF -
AGC(I)-99.
+
IF 0
GO TO 41
4
N=I-1
TUM=DAYN+H/24.0+FM/1440.
NYYN=DAYN
NM=(H*100.)+FM
I=0
53
I=I+1
READ
READ 54,IDAY,HRS,FMIN,GNAGC(I),HA(I),DEC(I)

DIMENSION AGC(25),PSN(25),YDB(5),ATT(5),ERR(25),

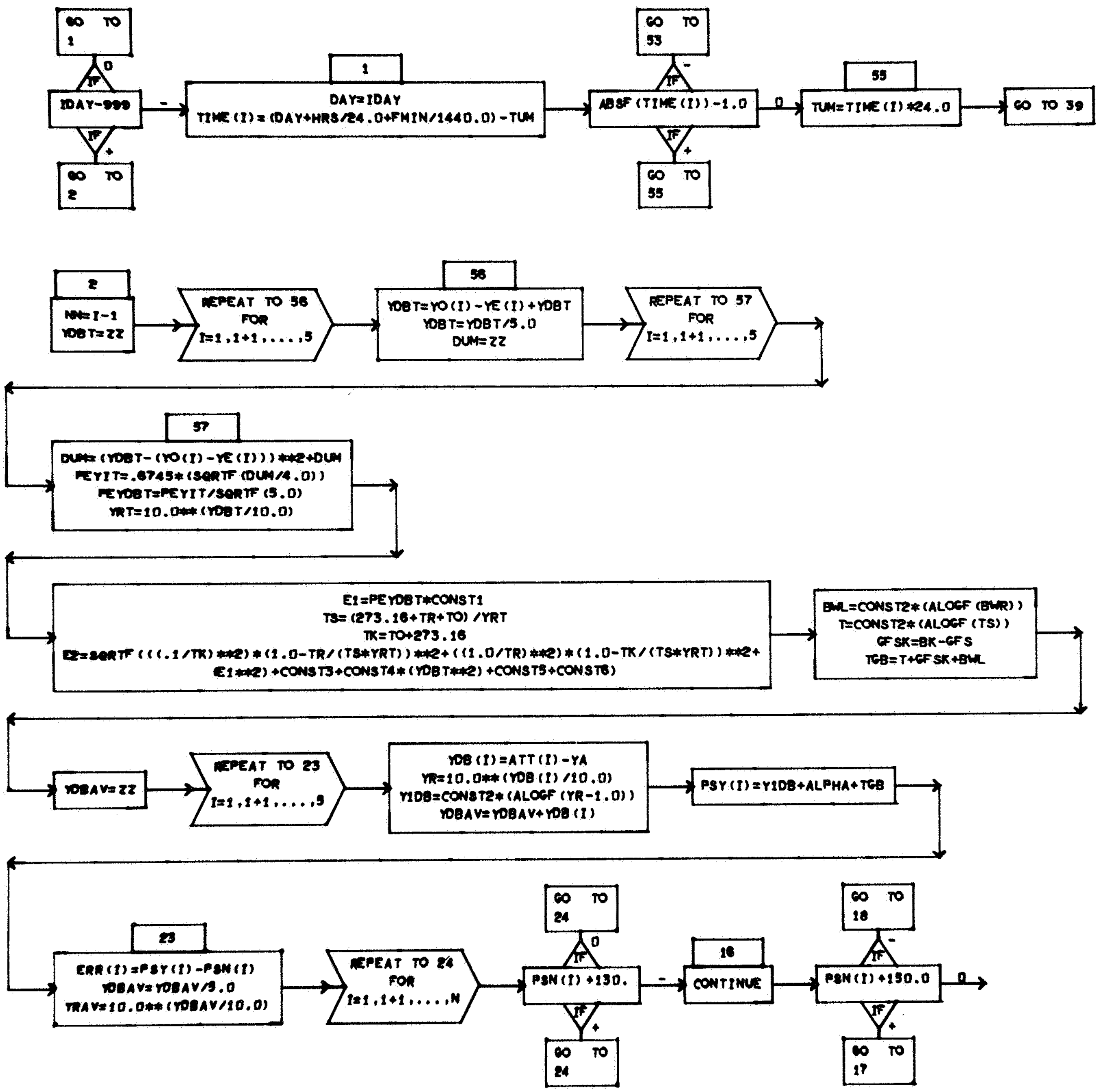

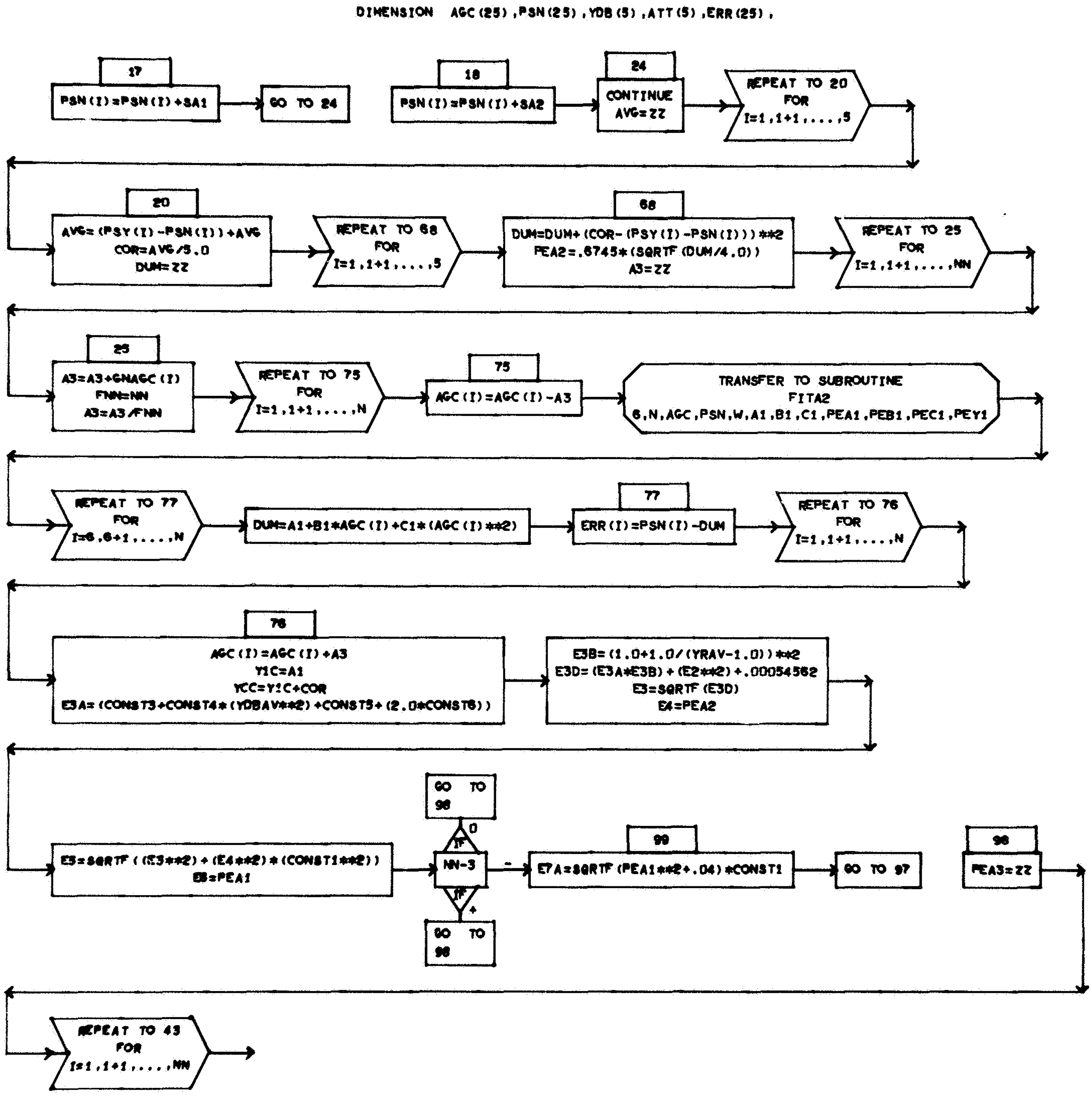
DIMENSION AGC(25),PSN(25),YDB(5),ATT(5),ERR(25),
17
PSN(I)=PSN(I)+SA1
GO TO 24
18
PSN(I)=PSN(I)+SA2
24
CONTINUE
AVG=ZZ
REPEAT TO 20
FOR
I=1,1+1,....,5
20
AVG=(PSY(I)-PSN(I))+AVG
COR=AVG/5.0
DUM=ZZ
REPEAT TO 68
FOR
I=1,1+1,....,5
68
DUM=DUM+(COR-(PSY(I)-PSN(I)))**2
PEA2=.6745*(SQRTF(DUM/4.0))
A3=ZZ
REPEAT TO 25
FOR
I=1,1+1,....,NN
25
A3=A3+GNAGC(I)
FNN=NN
A3=A3/FNN
REPEAT TO 75
FOR
I=1,1+1,....,N
75
AGC(I)=AGC(I)-A3
TRANSFER TO SUBROUTINE
FITA2
6,N,AGC,PSN,W,A1,B1,C1,PEA1,PEB1,PEC1,PEY1
REPEAT TO 77
FOR
I=6,6+1,....,N
DUM=A1+B1*AGC(I)+C1*(AGC(I)**2)
77
ERR(I)=PSN(I)-DUM
REPEAT TO 76
FOR
I=1,1+1,....,N
76
AGC(I)=AGC(I)+A3
Y1C=A1
YCC=Y1C+COR
E3A=(CONST3+CONST4*(YDBAV**2)+CONST5+(2.0*CONST6))
E3B=(1.0+1.0/(YRAV-1.0))**2
E3D=(E3A*E3B)+(E2**2)+.00054562
E3=SQRTF(E3D)
E4=PEA2
E5=SQRTF((E3**2)+(E4**2)*(CONST1**2))
E6=PEA1
GO TO
98
0
IF
NN-3
IF
+
-
GO TO
98
99
E7A=SQRTF(PEA1**2+.04)*CONST1
GO TO 97
98
PEA3=ZZ
REPEAT TO 43
FOR
I=1,1+1,....,NN

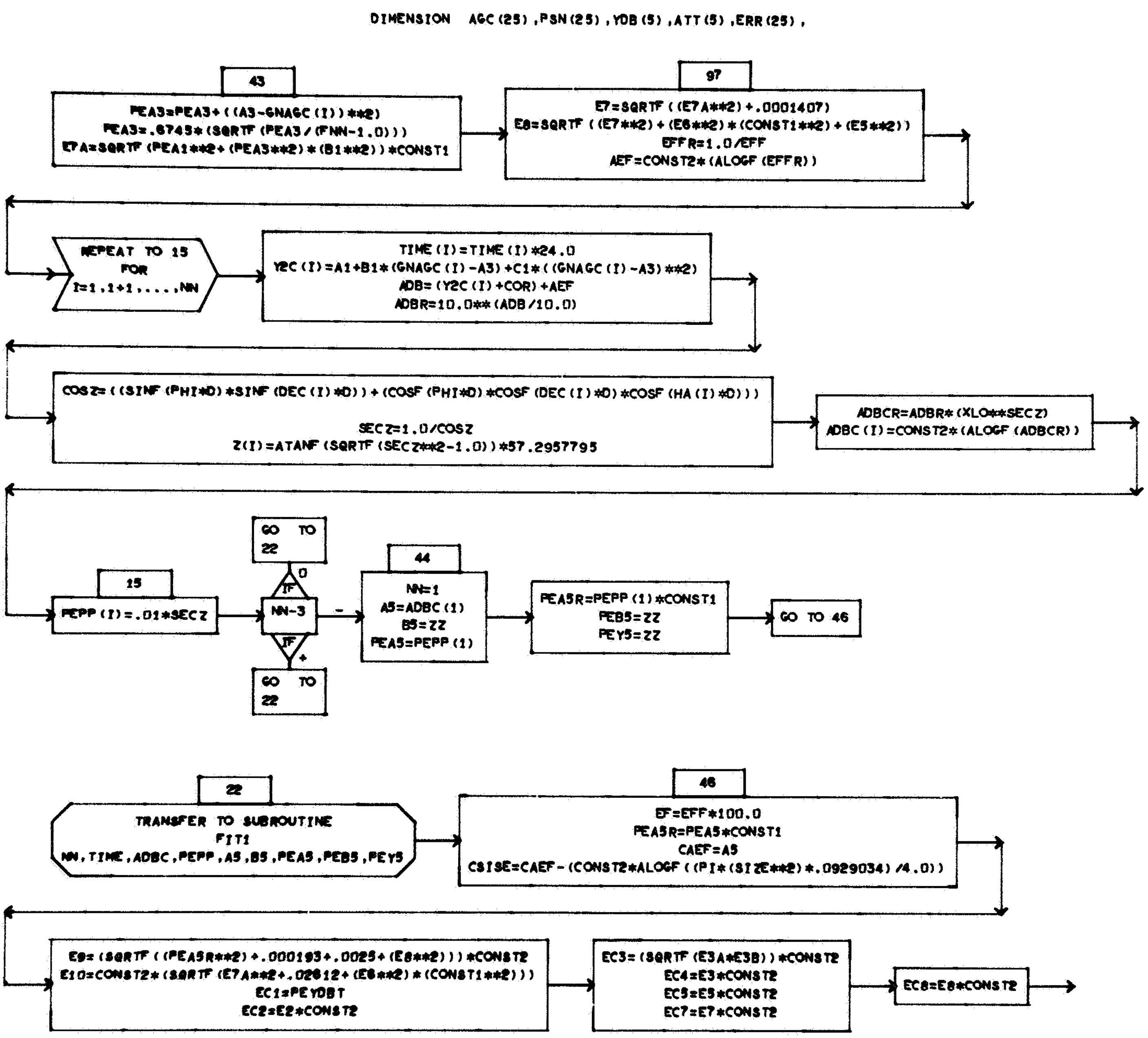

DIMENSION AGC (25) ,PSN (25) ,YDB (5) ,ATT (5) ,ERR (25) ,
43
PEA3=PEA3+((A3-GNAGC(I))**2)
PEA3=.6745*(SQRTF(PEA3/(FNN-1.0)))
E7A=SQRTF(PEA1**2+(PEA3**2)*(B1**2))*CONST1
97
E7=SQRTF((E7A**2)+.0001407)
E8=SQRTF((E7**2)+(E6**2)*(CONST1**2)+(E5**2))
EFFR=1.0/EFF
AEF=CONST2*(ALOGF(EFFR))
REPEAT TO 15
FOR
I=1,1+1,....,NN
TIME(I)=TIME(I)*24.0
Y2C(I)=A1+B1*(GNAGC(I)-A3)+C1*((GNAGC(I)-A3)**2)
ADB=(Y2C(I)+COR)+AEF
ADBR=10.0**(ADB/10.0)
COSZ=((SINF(PHI*D)*SINF(DEC(I)*D))+(COSF(PHI*D)*COSF(DEC(I)*D)*COSF(HA(I)*D)))
SECZ=1.0/COSZ
Z(I)=ATANF(SQRTF(SECZ**2-1.0))*57.2957795
ADBCR=ADBR*(XLO**SECZ)
ADBC(I)=CONST2*(ALOGF(ADBCR))
15
PEPP(I)=.01*SECZ
GO TO 22
0
IF
NN-3
IF
+
-
GO TO 22
44
NN=1
A5=ADBC(1)
B5=ZZ
PEA5=PEPP(1)
PEA5R=PEPP(1)*CONST1
PEB5=ZZ
PEY5=ZZ
GO TO 46
22
TRANSFER TO SUBROUTINE
FIT1
NN,TIME,ADBC,PEPP,A5,B5,PEA5,PEB5,PEY5
46
EF=EFF*100.0
PEA5R=PEA5*CONST1
CAEF=A5
CSISE=CAEF-(CONST2*ALOGF((PI*(SIZE**2)*.0929034)/4.0))
E9=(SQRTF((PEA5R**2)+.000193+.0025+(E8**2)))*CONST2
E10=CONST2*(SQRTF(E7A**2+.02612+(E8**2)*(CONST1**2)))
EC1=PEYDBT
EC2=E2*CONST2
EC3=(SQRTF(E3A*E3B))*CONST2
EC4=E3*CONST2
EC5=E5*CONST2
EC7=E7*CONST2
EC8=E8*CONST2

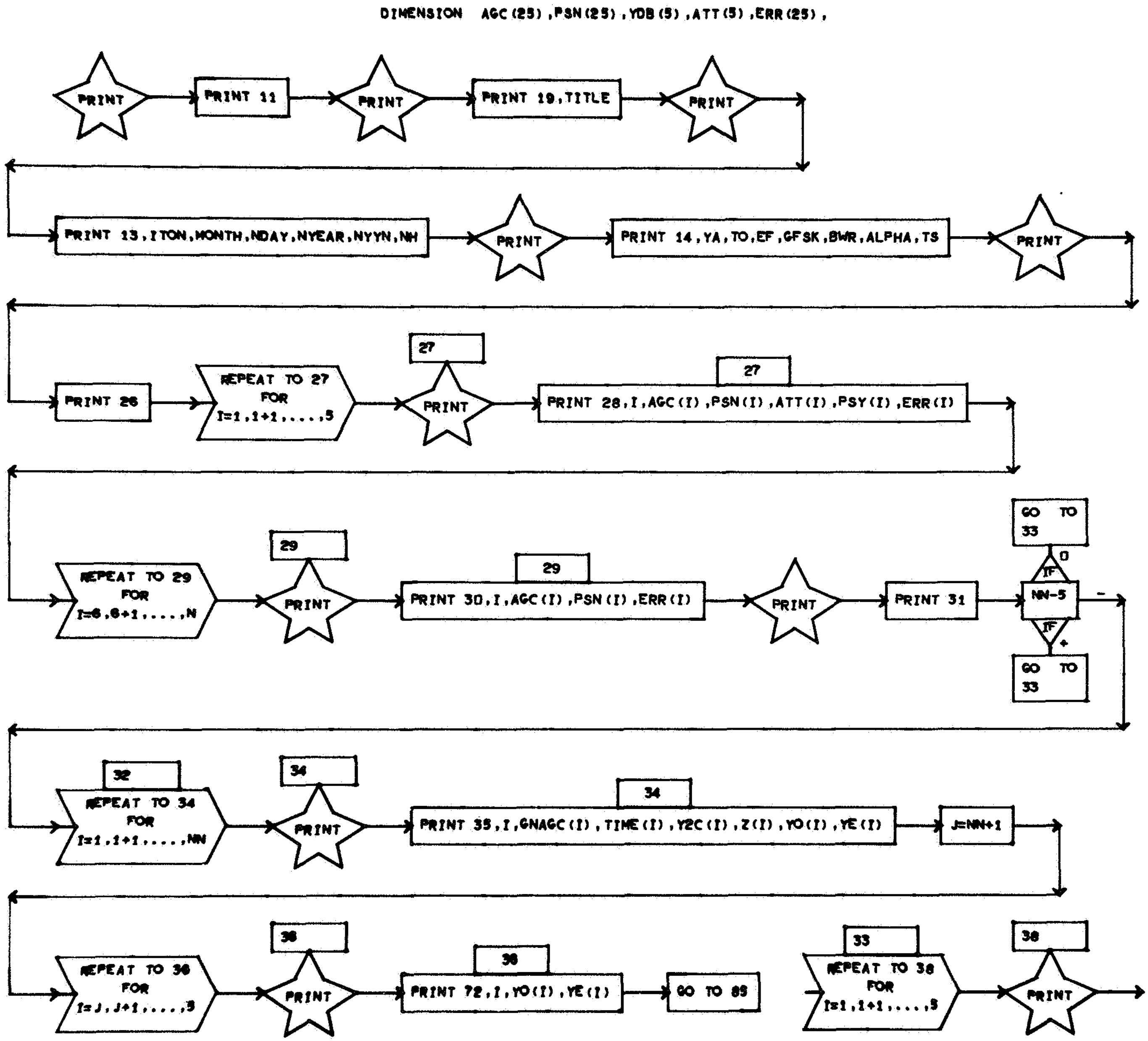
DIMENSION AGC(25),PSN(25),YDB(5),ATT(5),ERR(25),
PRINT
PRINT 11
PRINT
PRINT 19,TITLE
PRINT
PRINT 13,ITON,MONTH,NDAY,NYEAR,NYYN,NH
PRINT
PRINT 14,YA,TO,EF,GFSK,BWR,ALPHA,TS
PRINT
PRINT 26
REPEAT TO 27 FOR I=1,1+1,....,5
27
PRINT
27
PRINT 28,I,AGC(I),PSN(I),ATT(I),PSY(I),ERR(I)
REPEAT TO 29 FOR I=6,6+1,....,N
29
PRINT
29
PRINT 30,I,AGC(I),PSN(I),ERR(I)
PRINT
PRINT 31
GO TO 33
0
IF
NN-5
IF
+
-
GO TO 33
32
REPEAT TO 34 FOR I=1,1+1,....,NN
34
PRINT
34
PRINT 35,I,GNAGC(I),TIME(I),Y2C(I),Z(I),YO(I),YE(I)
J=NN+1
REPEAT TO 36 FOR I=J,J+1,....,5
36
PRINT
36
PRINT 72,I,YO(I),YE(I)
GO TO 85
33
REPEAT TO 38 FOR I=1,1+1,....,5
38
PRINT

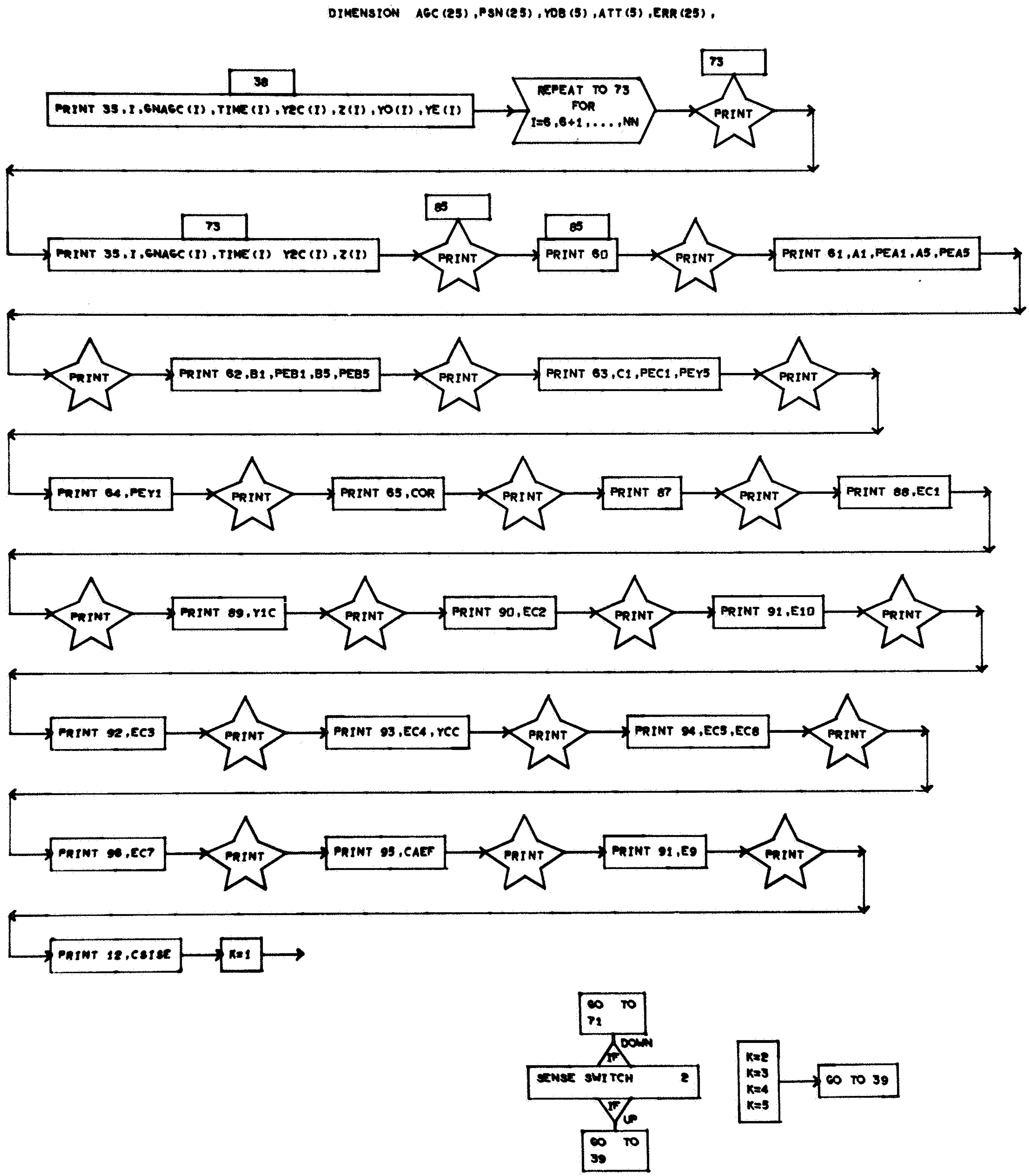

DIMENSION AGC(25),PSN(25),YOB(5),ATT(5),ERR(25),
38
PRINT 35,I,GNAGC(I),TIME(I),Y2C(I),Z(I),YO(I),YE(I)
REPEAT TO 73 FOR I=6,6+1,....,NN
73
PRINT
73
PRINT 35,I,GNAGC(I),TIME(I) Y2C(I),Z(I)
85
PRINT
85
PRINT 60
PRINT
PRINT 61,A1,PEA1,A5,PEA5
PRINT
PRINT 62,B1,PEB1,B5,PEB5
PRINT
PRINT 63,C1,PEC1,PEY5
PRINT
PRINT 64,PEY1
PRINT
PRINT 65,COR
PRINT
PRINT 87
PRINT
PRINT 88,EC1
PRINT
PRINT 89,Y1C
PRINT
PRINT 90,EC2
PRINT
PRINT 91,E10
PRINT
PRINT 92,EC3
PRINT
PRINT 93,EC4,YCC
PRINT
PRINT 94,EC5,EC8
PRINT
PRINT 96,EC7
PRINT
PRINT 95,CAEF
PRINT
PRINT 91,E9
PRINT
PRINT 12,CSISE
K=1
GO TO 71
DOWN
IF
SENSE SWITCH 2
IF
UP
GO TO 39
K=2
K=3
K=4
K=5
GO TO 39

D I M E N S I O N E D   V A R I A B L E S

SYMBOL	STORAGES	SYMBOL	STORAGES	SYMBOL	STORAGES	SYMBOL	STORAGES	SYMBOL	STORAGES
X	15	Y	15	W	15				

SUBROUTINE FIT1 (N,X,Y,W,A,B,PEA,PEB,PEY)

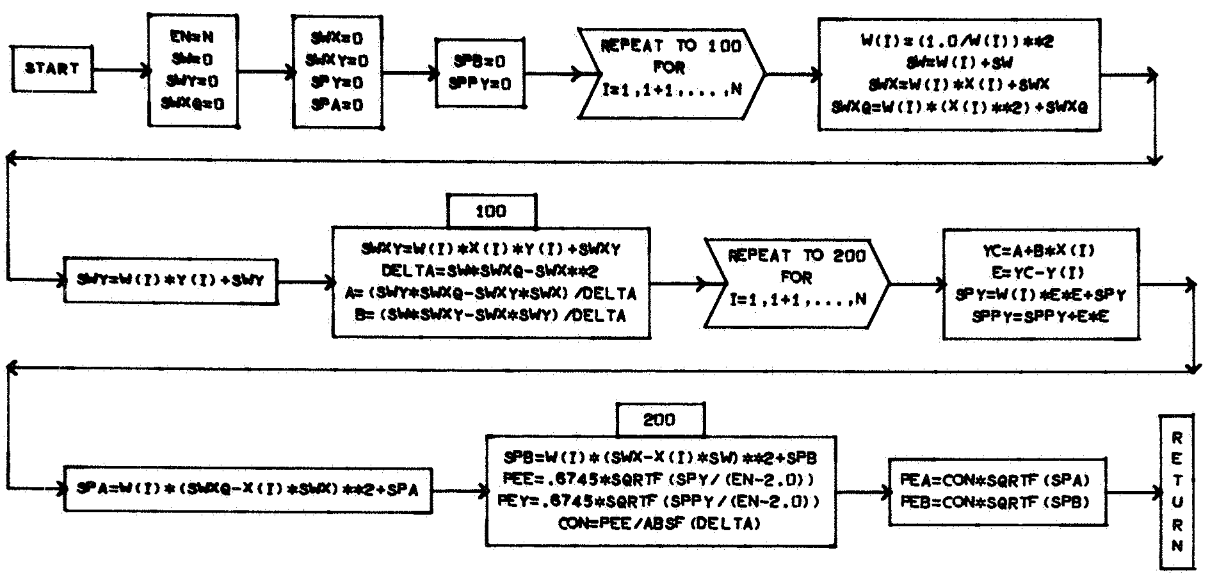

D I M E N S I O N E D   V A R I A B L E S

SYMBOL	STORAGES	SYMBOL	STORAGES	SYMBOL	STORAGES	SYMBOL	STORAGES	SYMBOL	STORAGES
X	100	Y	100	W	100				

SUBROUTINE FITA2 (NS,N,X,Y,W,A,B,C,PEA,PEB,PEC,PEY)

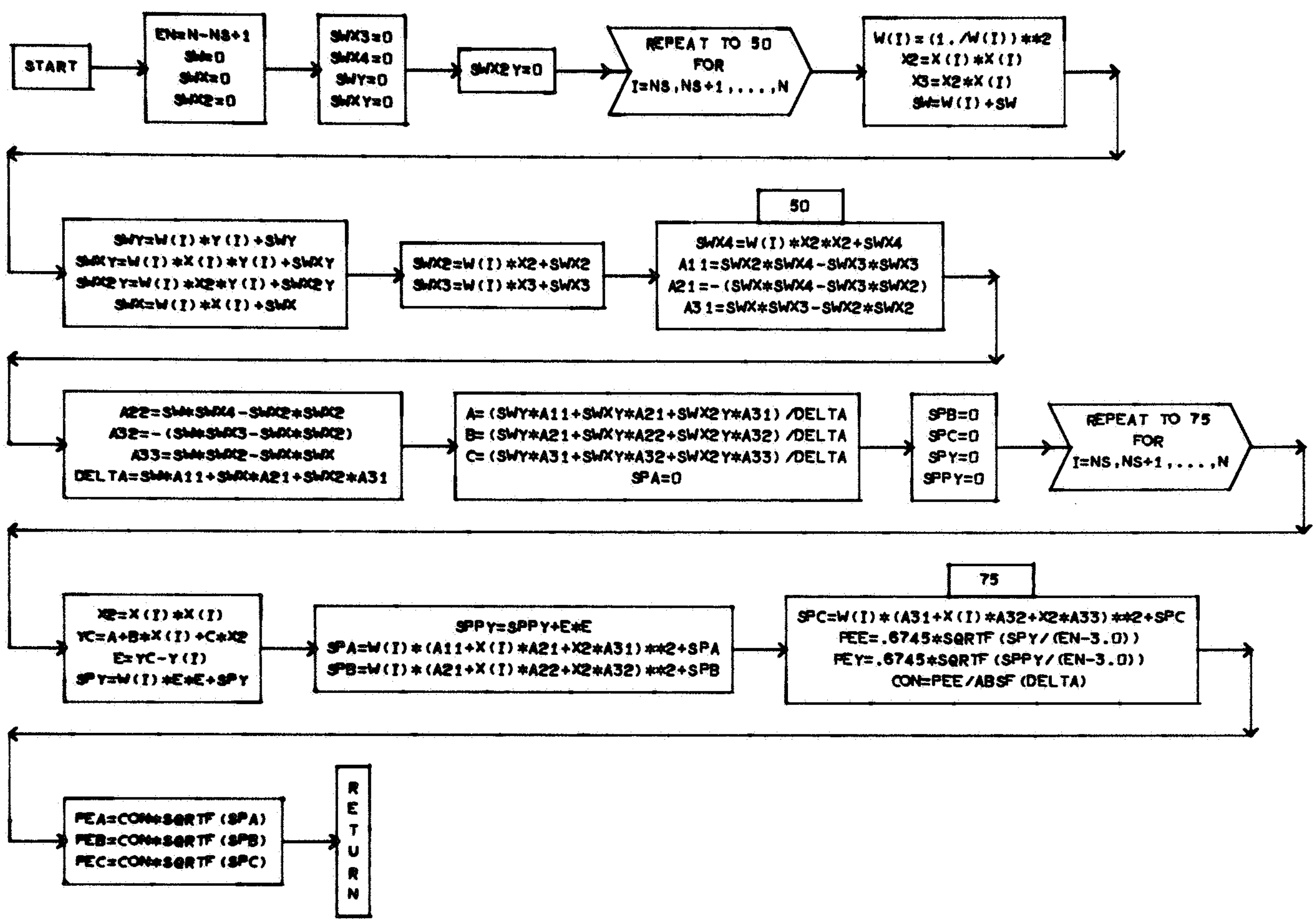

Nomenclature

(1) Text

- a proportionality factor associated with the detector law, ratio
- a_1 precision IF attenuator resettability constant, ratio
- a_2 precision IF attenuator linearity constant, ratio
- a_3 receiving system nonlinearity, RF to IF, ratio
- a_4 nonlinearity and calibration of the variable attenuator in the test transmitter, ratio
- a_5 calibration of the step attenuator in the test transmitter, ratio
- a_6 AGC voltage indicator jitter, ratio
- a_7 antenna-to-spacecraft pointing error, ratio
- A antenna aperture, m^2
- A_i i^{th} coefficient of the power series in the expansion of detector current in terms of the voltage across the detector, mhos
- A_1 constant of the best fit second-order curve defining the computed nominal AGC curve, dBmW
- A_3 average value of the GNAGC data points, V
- A_5 constant of the computed straight line fitted to the incident power data versus normalized time of measurement, dBmW
- b test transmitter linearity constant, ratio
- B equivalent noise bandwidth, Hz
- B_d overall equivalent noise bandwidth with diode detector, Hz
- B_p overall equivalent noise bandwidth with true rms detector, Hz
- B_1 constant of the best fit second-order curve defining the computed nominal AGC curve, dBmW/V
- B_5 constant of the computed straight line fitted to the incident power data versus normalized time of measurement, dBmW/day
- C effective shunt capacitance in the detector system equivalent circuit, F
- C_i i^{th} coefficient of the power series in the expansion of detector current in terms of the circuit input voltage, mhos
- COR correction factor for the calibration of the test transmitter power levels, dB
- C_1 constant of the best fit second-order curve defining the computed nominal AGC curve, dBmW/(V)^2
- e detector circuit ac input voltage, V
- E_n output indicator response caused by a detector input of noise power alone, V
- E_{sn} output indicator response caused by a detector input of signal combined with noise, V
- $(E_0)_n$ average (detector) dc output voltage caused by a noise input voltage, V
- $(E_0)_s$ average (detector) dc output voltage caused by a signal input voltage, V
- f_i frequency of the i^{th} data point, Hz
- f_s signal frequency, Hz
- ${}_1F_1$ confluent hypergeometric function
- $g(f_s)$ overall normalized system gain at frequency f_s, ratio
- $G(f)$ overall system gain at frequency f, ratio
- $G(f_s)$ overall system gain at frequency f_s, ratio
- $G(f_0)$ maximum overall system gain, ratio
- $GNAGC$ the data points of receiver AGC voltage on the spacecraft, V
- $\frac{\Delta G}{G_0}$ statistical overall receiver gain ratio fluctuations
- h radio source or spacecraft hour angle, deg
- I_s signal current, A
- I_n noise current, A
- k Boltzmann's constant, J/°K

Nomenclature (contd)

L_n IF attenuation in the Y-factor determination of α for an input consisting of noise power alone, ratio

L_{sn} IF attenuation in the Y-factor determination of α for an input consisting of signal combined with noise, ratio

L_0 assumed atmospheric loss at zenith, ratio

n number of data points in the determination of bandwidth

N number of nominal AGC curve data points; also, number of terms in the power series expansions of diode current

N' number of measured Y-factors in the determination of system temperature

NN number of data points of receiver AGC voltage on the spacecraft; i.e., number of GNAGC data points

P_n system noise power observed at the output of the narrow-band filter, W

P_s CW signal power observed at the output of the narrow-band filter, W

P_{si} spacecraft signal power defined at the receiver input reference plane, W

P^*_{si} test transmitter input signal power defined at the receiver input reference plane, W

P'_{si} calibrated spacecraft signal power incident on the antenna, W

P''_{si} calibrated spacecraft signal power which would be incident on the antenna with atmospheric loss removed, W

ΔP^*_{si} statistical test transmitter power gain fluctuations, W

P_{sn} detector system input power consisting of signal combined with noise, W

$(P_n)_i$ detector input power consisting of noise power alone, W

$(P_{sn})_i$ detector input power consisting of signal combined with noise, W

PE_{se} the effective probable error arising from the summation of the error terms a_3 through a_7, ratio

PE_{TTC} probable error of the test transmitter calibration (nominal method), dB

PE_x probable error of the arbitrary independent variable x

$PE_{y_{a0}}/y_{a0}$ probable error ratio. It is an error term which arises from the measurement scatter on the Y-factors in the determination of system temperature, and is one of the error terms which contribute to the probable error ratio $PE_{Y_{a0}}/Y_{a0}$

R effective diode load resistance, ohms

T assumed radio source temperature, °K

T' measured radio source temperature, °K

T_0 ambient temperature, °K

T_r receiver effective noise temperature defined at the receiver input reference plane, °K

T_s system effective noise temperature defined at the receiver input reference plane, °K

T_{sa} system effective noise temperature, defined at the receiver input reference plane, with a radio source outside the antenna beam, °K

T_{ss} system effective noise temperature, defined at the receiver input reference plane, with the antenna on a radio source, °K

v rms voltage, V

V peak voltage, V

w weighting factor in the statistical determination of the best straight line fitted to the incident power data versus normalized time of measurement, ratio

x arbitrary independent variable

y_i relative gain corresponding to frequency f_i, ratio

Y measurement power ratio obtained by turning the test transmitter off and on

Y_{a0} measurement power ratio obtained by switching between the antenna at zenith and the ambient load

Y_d same as Y with a diode detector

Nomenclature (contd)

Y_{dB} measurement power ratio in decibels

Y_p same as Y with a true rms detector

Y_1 measurement power ratio obtained by switching between the antenna on a radio source and the ambient load

Y_2 measurement power ratio obtained by switching between the antenna off a radio source and the ambient load

z radio source or spacecraft zenith angle, deg

α diode detector correction factor, ratio

β proportionality ratio of output indicator response under the condition $E_{sn}/E_n = 1$

β' generalized proportionality ratio of output indicator response with detector inputs of signal combined with noise and noise power alone

Γ gamma function

δ radio source or spacecraft declination, deg

η antenna efficiency defined at the receiver input, ratio

ν generalized detector law

σ standard deviation

τ post-detector time constant, s

ϕ antenna latitude, deg

(2) Program

Program	Text	
ADB		NN values of received spacecraft power, calibrated and normalized for 100% antenna efficiency, dBmW
ADBC	P''_{si}	calibrated spacecraft signal power which would be incident on the antenna with atmospheric loss removed, dBmW
ADBCR		NN values of calibrated spacecraft signal power which would be incident on the antenna with atmospheric loss removed, ratios
ADBR		ADB expressed as ratios
AEF		reciprocal of antenna efficiency, dB
AGC		AGC voltage readings for the calibration of the test transmitter, V
ALPHA	α	diode detector correction factor, ratio
ATT		IF attenuator levels for the calibration of the test transmitter, dB
A1	A_1	constant of the best fit second-order curve defining the computed nominal AGC curve, dBmW
A3	A_3	average value of the GNAGC data points, V. This is the reference point to which the Y-axis is transformed
A5	A_5	constant of the computed straight line fitted to the incident power data versus normalized time of measurement, dBmW

Nomenclature (contd)

BK	k	Boltzmann's constant, J/°K.
BWL		equivalent noise bandwidth of narrow-band filter, dB
BWR	B	equivalent noise bandwidth of narrow-band filter, Hz
B1	B_1	constant of the best fit second-order curve defining the computer nominal AGC curve, dBmW/V
B5	B_5	constant of the computed straight line fitted to the incident power data versus normalized time of measurement, dBmW/day
CAEF		incident power, dBmW
CONST 1		ln 10/10
CONST 2		10/ln 10
CONST 3	$(a_1)^2$	0.47717×10^{-6}, squared ratio
CONST 4	$(a_2)^2$	0.6626×10^{-6}, (ratio/dB)^2
CONST 5	$1/\tau B$	10^{-5}, ratio
CONST 6	$\left\{ \begin{matrix} \left(\frac{\Delta G}{G_0}\right)^2 \\ \frac{\Delta P^*_{si}}{P^*_{si}} \end{matrix} \right.$	2.5×10^{-6}, squared ratio
COR	COR	power correction factor, dB
CORR		heading under which the ERR differences are printed
CSISE		incident power density; received signal strength per m^2 of antenna aperture, dBmW/m^2
C1	C_1	constant of the best fit second-order curve defining the computed nominal AGC curve, dBmW/(V)^2
D		conversion factor; converts radians to deg
DAYN		day of year (calibration time)
DEC	δ	radio source or spacecraft declination, deg
EF		antenna efficiency expressed as a percentage
EFF	η	antenna efficiency defined at the receiver input, ratio
EFFR		reciprocal of antenna efficiency, ratio
ERR		the differences between the nominal and calibrated test transmitter power levels, dB
E2	PE_{T_s}/T_s	probable error of the system temperature measurement, ratio

Nomenclature (contd)

E4	PE_{A_2}	probable error of the calibration of the test transmitter signal level by the microwave thermal standards method; excluding measurement scatter of data points, ratio
E5		probable error of the calibration of the test transmitter level by the microwave thermal standards method, ratio
E6	PE_{A_1}	error contribution caused by the measurement scatter on the nominal AGC curve, ratio
E7		that portion of the probable error of the nominal spacecraft power which is common to both nominal and microwave thermal standards methods, ratio
E8		probable error of the calibrated spacecraft power, ratio
E9		probable error of the incident power, dB
E10		probable error of the nominal spacecraft power, dB
EC1		measurement error associated with the Y-factors in the determination of system temperature, dB
EC2		probable error of the computed system temperature, dB
EC3		Y-factor error contribution to the calibration of the test transmitter by the microwave thermal standards method, dB
EC4		probable error of the calibration of the test transmitter signal level by the microwave thermal standards method, excluding measurement scatter of data points, dB
EC5		complete probable error of the calibration of the test transmitter by the microwave thermal standards method, dB
EC6		error contribution caused by the measurement scatter on the nominal AGC curve, dB
EC7		that portion of the probable error of the nominal spacecraft power which is common to both the nominal method and the microwave thermal standards method, dB
EC8		probable error of the calibrated spacecraft power, dB
FM		minutes

Nomenclature (contd)

FIT 1		first-order best-fit subroutine
FIT A2		second-order best-fit subroutine
FNN and NN	NN	number of data points of receiver AGC voltage on the spacecraft
GFS	$g(f_s)$	overall normalized system gain at frequency f_s, ratio
GFSK	$k/g(f_s)$	ratio
GNAGC	$GNAGC$	data points of receiver AGC voltage on the spacecraft, V
H		hours
HA	h	radio source or spacecraft hour angle, deg
I	i	running index
IDAY		day of year (spacecraft power measurement time)
ITON		station number
MONTH, NDAY, NYEAR		date
PEA1	PE_{A_1}	probable error of the first constant of the best fit second-order curve defining the computed nominal AGC curve, dB
PEA2	PE_{A_2}	probable error of the correction factor COR, dB
PEA3	PE_{A_3}	probable error of the average value of the $GNAGC$ data points, V
PEA5	PE_{A_5}	probable error of the first constant of the computed straight line fitted to the incident power data versus normalized time of measurement, dB
PEA5R		PE_{A_5} expressed as a ratio
PEB1	PE_{B_1}	probable error of the second constant of the best fit second-order curve defining the computed nominal AGC curve, dB/V
PEB5	PE_{B_5}	probable error of the second constant of the computed straight line fitted to the incident power data versus normalized time of measurement, dB/day
PEC1	PE_{C_1}	probable error of the third constant of the best fit second-order curve defining the computed nominal AGC curve, dB/(V)^2
PEPP	w	weighting factor, ratio

Nomenclature (contd)

PEYDBT	$PE_{Y_{a0}}$	probable error of the average system temperature Y-factor, dB
PEY1T		intermediate step in the computation of PEYDBT, dB
PHI	ϕ	antenna latitude, deg
PSN		nominal test transmitter levels, dBmW
PI	π	
PSY		calibrated test transmitter power levels, dBmW
SA1, SA2		test transmitter step attenuator calibrations, dB
SIZE		antenna effective diameter, ft
T		system temperature in decibels
TGB	$\frac{kT_sB}{g(f_s)}$	
TK	T_0	ambient temperature, °K
TO		ambient temperature, °C
TR	T_r	receiver effective noise temperature, °K
TS	T_s	system effective noise temperature defined at the receiver input, °K
XLO	L_0	assumed value of atmospheric loss at zenith, 0.05 dB
YA		IF attenuator reference level for the measurement of T_s, dB
YCC	P'_{si}	calibrated spacecraft signal power defined at the receiver input reference plane, dBmW
YDB		measurement power ratio obtained by turning the test transmitter off and on, dB
YDBAV		the average calibration Y-factor, dB
YDBT		average measurement power ratio obtained by switching between the antenna at zenith and the ambient load, dB
YE, YO		IF attenuator levels for the measurement of system temperature, dB
YR	Y	measurement power ratio obtained by turning the test transmitter off and on
YRAV		the average calibration Y-factor, ratio
YRT	$\overline{Y}_{a0}$	YDBT expressed as a ratio

Nomenclature (contd)

Y1C		nominal value of received spacecraft power, dBmW
Y2C		*NN* values of nominal spacecraft power corresponding to *NN* values of receiver AGC voltage on the spacecraft, dBmW
Z	z	radio source or spacecraft zenith angle, deg

References

1. Stelzried, C. T., Reid, M. S., *Continuous Wave (CW) Signal Power Calibration With Thermal Noise Standards,* Space Programs Summary 37-38, Vol. III, p. 41, Jet Propulsion Laboratory, Pasadena, California, March 1966.

2. Stelzried, C. T., "Temperature Calibration of Microwave Thermal Noise Sources," *IEEE Trans. Microwave Theory and Techniques,* Vol. MTT-13, No. 1, Jan. 1965.

3. Sees, J. E., *Fundamentals in Noise Source Calibrations at Microwave Frequencies,* NRL Report 5051, Radio Astronomy Branch, Atmosphere and Astrophysics Division, Naval Research Laboratory, Washington, D.C., p. 5, Jan. 1958.

4. Reid, M. S., Stelzried, C. T., *Error Analysis of CW Signal Power Calibration with Thermal Noise Standards,* Space Programs Summary 37-36, Vol. IV, p. 268, Jet Propulsion Laboratory, Pasadena, California, Dec. 1965.

5. Tuiri, M. E., "Radio Astronomy Receivers," *IEEE Trans. Military Electronics,* Vol. MIL–8, Nos. 3 and 4, p. 267, July–Oct., 1964.

6. Reid, M. S., Stelzried, C. T., *CW Signal Power Calibration With Thermal Noise Standards,* Space Programs Summary 37-36, Vol. III, p. 44, Jet Propulsion Laboratory, Pasadena, California, Nov. 1965.

7. Stelzried, C. T., Reid, M. S., *Continuous Wave Signal Power Calibration With Thermal Noise Standards,* Space Programs Summary 37-39, Vol. III, p. 81, Jet Propulsion Laboratory, Pasadena, California, May 1966.

8. Stelzried, C. T., Reid, M. S., *CW Signal Power Calibration With Thermal Noise Standards,* Space Programs Summary 37-35, Vol. III, p. 58, Jet Propulsion Laboratory, Pasadena, California, Sept. 30, 1965.

9. Mathison, R. P., "*Mariner* Mars 1964 Telemetry and Command System," *IEEE Spectrum,* Vol. 2, No. 7, p. 76, July 1965.

10. Davenport, W. B., Root, W. L., *An Introduction to the Theory of Random Signals and Noise,* p. 304, McGraw-Hill Book Co., Inc., New York, 1958.

References (contd)

11. Davenport, W. B., Root, W. L., *An Introduction to the Theory of Random Signals and Noise*, p. 307, McGraw-Hill Book Co., Inc., New York, 1958.
12. Pipes, L. A., *Applied Mathematics for Engineers and Physicists*, p. 304, McGraw-Hill Book Co., Inc., New York, 1946.
13. Bennett, W. R., "Methods of Solving Noise Problems," *Proc. IRE*, Vol. 44, No. 5, p. 614, May 1956.